Elsevier Editorial System(tm) for Lithos
Manuscript Draft

Manuscript Number: LITHOS6949R1

Title: Phengite megacryst quasi-exsolving phlogopite, from Sulu Ultra-high Pressure Metamorphic Terrane, Qinglongshan, Donghai County (eastern China): new data for P-T-X conditions during exhumation.

Article Type: Regular Article

Keywords: phengite and phlogopite micas; exolution reactions; Sulu UHP metamorphic terrane; alkali-alumino-silicate high pressure fluids.

Corresponding Author: Dr. Costanza Bonadiman, PhD

Corresponding Author's Institution: University of Ferrara

First Author: Nadia Curetti

Order of Authors: Nadia Curetti; Costanza Bonadiman, PhD; Roberto Compagnoni; Luca Nodari; Indrid Corazzari; Alessandro Pavese

Abstract: A large crystal of trigonal phengite (Phe-3T; $K_{0.96}Na_{0.02}Ba_{0.01})(Al_{1.35}Mg_{0.40}Fe^{2+}_{0.11}Fe^{3+}_{0.13}Ti_{0.02})\Sigma=2.02[Si_{3.44}Al_{0.56}]O_{10}(OH)_2$), sampled from a phengite+quartz metamorphic vein in the eclogites-bearing rocks of Sulu UHP metamorphic terrane, exhibits unusual thin lamellae of ferrian-aluminian trigonal/monoclinic phlogopite polytypes (Phl-3T: $(K_{0.78}Na_{0.01})(Mg_{1.48}Fe^{2+}_{0.39}Fe^{3+}_{0.45}Al_{0.30}Ti_{0.06})\Sigma=2.68[Si_{2.98}Al_{1.02}]O_{10}((OH)_{1.77}F_{0.23})$; Phl-1M: $(K_{0.85}Ca_{0.01})(Mg_{1.43}Fe^{2+}_{0.45}Fe^{3+}_{0.54}Al_{0.21}Ti_{0.06})\Sigma=2.69[Si_{2.88}Al_{1.12}]O_{10}((OH)_{1.99}F_{0.01})$). This assemblage is rarely observed in UHP eclogite-bearing rocks, and has never been reported before in the Sulu UHP metamorphic terrane. A detailed crystal-chemical characterisation of Phe-3T, Phl-3T and Phl-1M allowed the development of a thermodynamic model that estimates the P-T conditions of formation of such an assemblage and helps to understand the relationship between mica polytypes and a quartz dominated (silica oversaturated) system, which characterized the Sulu vein. Phe-3T varies in composition upon approaching Phl-3T/1M, showing a decrease of Si and Al and an increase of Fe and Mg contents. Observed phlogopites cannot be ascribed to bare exsolving processes, and require the involvement of a non-isochemical reaction, dominated by exsolution (quasi-exsolution process) in combination with a contribution from an "external chemical supplier" (most probably provided by circulating fluids). Mass balance calculations between the mineralogical assemblage of Sulu vein and the solute components of alkali-alumino-silicate high pressure fluids demonstrate that a silicic-type major element composition accounts for a phengite-quartz based rock. The occurrence of phlogopite micas can be explained as an effect of disproportion in combination with supply components, i.e. Mg, Al and K, from alkali-alumino-silicate high pressure fluids.
On the basis of energy modelling of the reaction process from phengite to phlogopite in presence of quartz and a matter exchanger, we determined that such a transformation is weakly dependent on T over the 500-930° C thermal range. The intersection of the calculated P-T assemblage equilibrium curve with the country rock P-T metamorphic path occurs at

P~2.4±0.2 GPa and T ~ 700° C, thus reflecting an early stage of exhumation, close to the metamorphic peak of the Sulu UHP terrane.

Revision Notes
Click here to download Revision Notes: Authors reply letter.docx

Dear Editor,

The revised version of the manuscript ‘ Phengite megacryst quasi-exsolving phlogopite, from Sulu Ultra-high Pressure Metamorphic Terrane, Qinglongshan, Donghai County (eastern China): new data for P-T-X conditions during exhumation.’’ has been uploaded.

First of all, the authors are honored to have got a positive feedback about this study from either reviewers, and editor.
We are also thankful for the rigorous editorial work they have paid to our manuscript. In this light, the authors have introduced all the corrections and enhancements suggested by the reviewers. Changes are in red, in the revised manuscript.

For the Authors

Costanza Bonadiman

COMMENTS FROM EDITORS AND REVIEWERS

Dear Dr. Bonadiman,
two reviews of your manuscript are now available. I am quite glad to see that the reviewer's comments are quite positive as they recommend publication after minor revision and/or acceptance of the paper in the present for.
Compliments for the interesting work.
I look forward to receive the revised manuscript to proceed with acceptance.
With kind regards

Marco Scambelluri
Lithos editor

Reviewer #1: The manuscript by Curetti et al. describes an un common assemblage of dioctahedral and trioctahedral micas with different polytypes, together with all the thermodynamic reactions leading to the formation of the mentioned assemblage.
The interesting results provided by authors and the sound scientific approach leading to their generation and interpretation deserve publication on Lithos. I certainly recommend publication after fixing some points, mainly related to form rather than to the scientific matter. Some points to be considered for correction are listed below.
Table S1 reports Suluphe instead of Phe-3T as reported throughout the text.

Authors’ reply: Thanks for noting. We change accordingly.

Several references reported in the manuscript are not reported in the reference list, e.g. Castelli et al. 1998; Gresen et al. 1971; Goodman 1976; Aldrige et al., 1987; Finch et al. 1982; Shabani et al.1998; Franz et al. 1987. Vice versa many quotations in reference list are not present in the text, e.g. Hermann, J., Rubatto, D., 2014; Ivaldi, G., Curetti, N., Gula, A., 2002; Frank, W., Höck, V., Miller, C.; Hermann, J., Rubatto, D., Korsakov, A., Shatsky, V.S., 2001; Pavese, A., 2002; Pavese, A., Diella, V., 2010; Shaw, D.M., 1970; Wallis, S., Tsuboi, M., Suzuki, K., Fanning, M., Jiang, L.L., Tanaka, T., 2005; Wallis, S., Ishiwatari, A., Hirajima, T., Ye, K., Guo, J., Nakamura, D., Kato, T., Zhai, M., Enami, M., Cong, B., and Banno, S., 1997; Zhang, R-Y., Liou, J.G., Shau, J.F., 2002; Zhang Z-M., Xiao Y-L., Liu F-L., Liou, J.G., and Hoefs, J., 2005; Zhao, Z-F., Zheng, Y-

F., Zhang, J., Dai, L.Q., Liu, X.M., 2012; Zheng, Y-F., 2012; Zheng, Y-F., Hermann, J., 2014; Zheng, Y-F, Xia, Q-X, Chen, R-X, Gao, X-Y., 2011.

Authors' reply: We apologize for this. It is attributable to the corresponding author who uploaded a preliminary reference-crosschecked version of the manuscript.
The revised version is complete and duly checked for references in each section. The missing references (both in the text and in the reference list) are in red.

Reviewer #2: The manuscript deals with a rare occurrence of phlogopite in phengite megacryst found in a phengite-quartz vein within the UHP Sulu metamorphic terrane. Profiting of a detailed crystal-chemical analysis including Mossbauer Spectroscopy for the determinationof Fe2+ and Fe3+ the authors propose a fluid-dominated reaction in an open metamorphic system that allow the formation of quasi-exsolving phlogopite. Thermodynamic modeling is then used to determine PT metamorphic conditions of an exhumation stage to be compared with reported metamorphic peak for the Sulu UHP terrane.

The manuscript is well written, the goal clearly explained and all the data well presented.
The topic is certainly of broad scientific interest and deserves to be published in Lithos almost in the present form.
In the following only few minor corrections.

Minor corrections:

lines 51-53: delete "usually hydrous"

Done

line 61: substitute "in dry conditions" with "at dry conditions"

Done
lines 62: move the reference (Poli and Fumagalli 2003) in the end of the sentence. As it is, it seems that Poli and Fumagalli stated that eclogites form at dry conditions.

Authors' reply: thanks for noting. We move the reference accordingly

Best regards.
Patrizia Fumagalli

Phengite megacryst *quasi*-exsolving phlogopite, from Sulu Ultra-high Pressure Metamorphic Terrane, Qinglongshan, Donghai County (eastern China): new data for *P-T-X* conditions during exhumation

Nadia Curetti[a], Costanza Bonadiman [b], Roberto Compagnoni[a,] Alessandro Pavese[a], Luca Nodari[c], Ingrid Corazzari[d,e]

[a] Department of Earth Sciences, University of Turin, 10125 Turin, Italy

[b] Department of Physics and Earth Sciences, University of Ferrara, 44122 Ferrara, Italy

[c] Institute of Condensed Matter Chemistry and Technology for the Energy– CNR – Padua, Italy

[d] Department of Chemistry, University of Turin, 10125 Turin, Italy

[e] "G. Scansetti" Interdepartmental Center for Studies on Asbestos and Other Toxic Particulates, Turin, Italy.

Abstract

A large crystal of trigonal phengite (*Phe-3T*; $K_{0.96}Na_{0.02}Ba_{0.01}(Al_{1.35}Mg_{0.40}Fe^{2+}_{0.11}Fe^{3+}_{0.13}Ti_{0.02})_{\Sigma=2.02}[Si_{3.44}Al_{0.56}]O_{10}(OH)_2$), sampled from a phengite+quartz metamorphic vein in the eclogites-bearing rocks of Sulu UHP metamorphic terrane, exhibits unusual thin lamellae of ferrian-aluminian trigonal/monoclinic phlogopite polytypes (*Phl-3T*: $(K_{0.78}Na_{0.01})(Mg_{1.48}Fe^{2+}_{0.39}Fe^{3+}_{0.45}Al_{0.30}Ti_{0.06})_{\Sigma=2.68}[Si_{2.98}Al_{1.02}]O_{10}((OH)_{1.77}F_{0.23})$; *Phl-1M*: $(K_{0.85}Ca_{0.01})(Mg_{1.43}Fe^{2+}_{0.45}Fe^{3+}_{0.54}Al_{0.21}Ti_{0.06})_{\Sigma=2.69}[Si_{2.88}Al_{1.12}]O_{10}((OH)_{1.99}F_{0.01})$).

This assemblage is rarely observed in UHP eclogite-bearing rocks, and has never been reported before in the Sulu UHP metamorphic terrane. A detailed crystal-chemical characterisation of *Phe-3T*, *Phl-3T* and *Phl-1M* allowed the development of a thermodynamic model that estimates the *P-T* conditions of formation of such an assemblage and helps to understand the relationship between mica polytypes and a quartz dominated (silica oversaturated) system, which characterized the Sulu vein. *Phe-3T* varies in composition upon approaching *Phl-3T*/*1M*, showing a decrease of Si and Al

and an increase of Fe and Mg contents. Observed phlogopites cannot be ascribed to bare exsolving processes, and require the involvement of a non-isochemical reaction, dominated by exsolution (*quasi*-exsolution process) in combination with a contribution from an "external chemical supplier" (most probably provided by circulating fluids). Mass balance calculations between the mineralogical assemblage of Sulu vein and the solute components of alkali-alumino-silicate high pressure fluids demonstrate that a silicic-type major element composition accounts for a phengite-quartz based rock. The occurrence of phlogopite micas can be explained as an effect of disproportion in combination with supply components, *i.e.* Mg, Al and K, from alkali-alumino-silicate high pressure fluids.

Phengite megacryst *quasi*-exsolving phlogopite, from Sulu Ultra-high Pressure Metamorphic Terrane, Qinglongshan, Donghai County (eastern China): new data for *P-T-X* conditions during exhumation.

by Nadia Curetti, Costanza Bonadiman, Roberto Compagnoni, Luca Nodari, Ingrid Corazzari, Alessandro Pavese

Highlights:

- Coexistence of phengite and phlogopite is rare and never observed in Sulu UHP metamorphic terrane.
- Exsolving reactions in open system to model a non-isochemical exsolution process.
- *Quasi*-exsolved phlogopite from disproportion and a supply of elements from HP fluids.
- *P-T locus* of phengite-phlogopite-quartz-fluid equilibrium close to the metamorphic peak.

Phengite megacryst *quasi*-exsolving phlogopite, from Sulu Ultra-high Pressure Metamorphic Terrane, Qinglongshan, Donghai County (eastern China): new data for *P-T-X* conditions during exhumation

Nadia Curetti[a], Costanza Bonadiman [b], Roberto Compagnoni[a,] , Luca Nodari[c], Ingrid Corazzari[d,e] , Alessandro Pavese[a]

[a] Department of Earth Sciences, University of Turin, 10125 Turin, Italy

[b] Department of Physics and Earth Sciences, University of Ferrara, 44122 Ferrara, Italy

[c] Institute of Condensed Matter Chemistry and Technology for the Energy– CNR – Padua, Italy

[d] Department of Chemistry, University of Turin, 10125 Turin, Italy

[e] "G. Scansetti" Interdepartmental Center for Studies on Asbestos and Other Toxic Particulates, Turin, Italy.

key-words: phengite and phlogopite micas, exolution reactions, Sulu UHP metamorphic terrane, alkali-alumino-silicate high pressure fluids.

corresponding author: Costanza Bonadiman (bdc @unife.it)

In memory of Prof. Xu Shutong

Abstract

A large crystal of trigonal phengite (*Phe-3T*; $K_{0.96}Na_{0.02}Ba_{0.01})(Al_{1.35}Mg_{0.40}Fe^{2+}_{0.11}Fe^{3+}_{0.13}Ti_{0.02})_{\Sigma=2.02}[Si_{3.44}Al_{0.56}]O_{10}(OH)_2$), sampled from a phengite+quartz metamorphic vein in the eclogites-bearing rocks of Sulu UHP metamorphic terrane, exhibits unusual thin lamellae of ferrian-aluminian trigonal/monoclinic phlogopite polytypes (*Phl-3T*: $(K_{0.78}Na_{0.01})(Mg_{1.48}Fe^{2+}_{0.39}Fe^{3+}_{0.45}Al_{0.30}Ti_{0.06})_{\Sigma=2.68}[Si_{2.98}Al_{1.02}]O_{10}((OH)_{1.77}F_{0.23})$; *Phl-1M*: $(K_{0.85}Ca_{0.01})(Mg_{1.43}Fe^{2+}_{0.45}Fe^{3+}_{0.54}Al_{0.21}Ti_{0.06})_{\Sigma=2.69}[Si_{2.88}Al_{1.12}]O_{10}((OH)_{1.99}F_{0.01})$). This assemblage is rarely observed in UHP eclogite-bearing rocks, and has never been reported before in the Sulu UHP metamorphic terrane. A detailed crystal-chemical characterisation of *Phe-3T*, *Phl-3T* and *Phl-1M* allowed the development of a thermodynamic model that estimates the *P-T* conditions of formation of such an assemblage and helps to understand the relationship between mica polytypes and a quartz dominated (silica oversaturated) system, which characterized the Sulu vein. *Phe-3T* varies in composition upon approaching *Phl-3T*/*1M*, showing a decrease of Si and Al and an increase of Fe and Mg contents. Observed phlogopites cannot be ascribed to bare exsolving processes, and require the involvement of a non-isochemical reaction, dominated by exsolution (*quasi*-exsolution process) in combination with a contribution from an "external chemical supplier" (most probably provided by circulating fluids). Mass balance calculations between the mineralogical assemblage of Sulu vein and the solute components of alkali-alumino-silicate high pressure fluids demonstrate that a silicic-type major element composition accounts for a phengite-quartz based rock. The occurrence of phlogopite micas can be explained as an effect of disproportion in combination with supply components, *i.e*. Mg, Al and K, from alkali-alumino-silicate high pressure fluids.

On the basis of energy modelling of the reaction process from phengite to phlogopite in presence of quartz and a matter exchanger, we determined that such a transformation is weakly dependent on *T* over the 500-930° C thermal range. The intersection of the calculated *P-T* assemblage equilibrium curve with the country rock *P-T* metamorphic path occurs at *P*~2.4±0.2 GPa and *T* ~ 700° C, thus reflecting an early stage of exhumation, close to the metamorphic peak of the Sulu UHP terrane.

1. Introduction

During prograde metamorphism, veins promoted by the availability of the fluid released by the dehydration reactions accompanying temperature (and pressure) increase are ubiquitous (Cong et al. 1994; Zheng et al., 2005). In case of decarbonation reactions, CO_2 also occurs in the fluid phase and carbonate minerals may form in place of or together with silicates. The vein mineral assemblage, which reflects the occurring *P-T-X* conditions at the time of its formation, is useful to infer the metamorphic path experienced by a rock during the whole tectonic evolution. Usually, a close relationship exists between the country rock and the mineralogical composition of the metamorphic vein: *e.g.*, in low-grade metapelites, most metamorphic veins consist of quartz and/or low-temperature minerals such as Fe-rich chlorite and epidote (Hermann and Rubatto, 2009).

Conversely to a widespread opinion that eclogites form at dry conditions or at very low water activity, metamorphic veins involving fluids are not unusual in the HP (high pressure) and UHP (ultra-high pressure) eclogite-facies (Poli and Fumagalli, 2003). For example, in eclogites quartz-rutile veins are ubiquitous, and they were used to estimate the metamorphic temperatures by means of the oxygen isotopes partitioning (*e.g.*, Desmons and O'Neill, 1978).

Good examples of such HP veins in subducted continental crust are found in the "Eclogitic Micaschist Complex" of the Sesia Zone, Western Alps, where quartz veins may include rutile crystals, more than 20 cm long (Compagnoni et al., 2014 and references therein). In the same unit, a metamorphic vein was found, 1-2 m thick and more than 80 m long, mainly consisting of phengite and minor quartz: the phengite flakes, which are up to 30 cm wide, show a unique oscillatory zoning and the coexistence of 3*T* and $2M_1$ polytypes, and no evidence of phlogopite polytypes (Ivaldi et al., 2001).

In the HP/UHP eclogites of the Dabie-Sulu orogenic belt, in addition to the ubiquitous quartz-rutile veins, quartz+zoisite+kyanite veins were found in the Zhu-Jia-Chong eclogite body, where the vein minerals may also attain a pegmatoid size (Castelli et al., 1998). It was proposed that such veins were formed in a closed system during the breakdown of lawsonite which resulted in a kyanite +zoisite +hydrous fluid, either before peak metamorphic conditions (Castelli et al., 1998) or during exhumation (Li et al., 2005).

These metamorphic veins are quite different from veins formed by partial melting during exhumation, which are characterised by a mineral assemblage that reflects the minimum melting granite, *i.e*. the ubiquitous presence of feldspars and mineral grain-size of the order of millimetres (Deng et al., 2017 and references therein).

The phengite specimen under investigation was sampled from a phengite+quartz metamorphic vein, excavated at Qinglongshan, very close to the G30 Lianhuo Expressway, crossing the Donghai County (eastern China). The phengite was collected in a small dump derived from a vertical shaft, excavated in the eclogites-bearing rocks of Sulu UHP metamorphic terrane to mine pure quartz (Fig. 1).

The peak conditions of the UHP metamorphism of the Qinglongshan rocks were estimated at T~700-800°C and P>2.8 GPa (Hirajima and Nakamura, 2003; Liu et al., 2015; Xu et al.,

2012; Zhang et al., 1995) and several *P-T* paths have been suggested (*e.g.*, Ferrando et al., 2005; Frezzotti et al., 2007).

The phengite sample consists of a single undeformed platy crystal, about 520 cm^3 in volume, with a dusky yellowish green colour (Rock Colour Chart, 1991), and it shows the unusual thin lamellae of Fe-phlogopite.

The coexistence of phengite and phlogopite is rarely observed in UHP eclogite-bearing rocks (*e.g.*, Eastern Alps; Eclogite Zone, Tauern, Austria; Frank et al.,1986) and, to the authors' knowledge, has never been reported from Sulu UHP terrane.

The condition and nature of the reactions that lead to the equilibrium of phengite with phlogopite (Zanazzi and Pavese, 2002) upon decreasing pressure are still poorly defined. Melting experiments, conducted on the synthetic K_2O-MgO-Al_2O_3-SiO_2-H_2O (KMASH) system (Massonne and Szpurka, 1997; Thomsen and Schmidt, 2008) and on natural carbonate-bearing eclogites (Droop et al., 1990; Zhang et al., 1995), suggest that a silicate melt at $P > 2$ kbar and $600° < T < 700°C$ produces volatile-rich phases, among which phengite plays a relevant role as potassic mineral (Hermann and Green, 2001; Massonne and Szpurka, 1997; Schmidt and Poli, 1998;; Schmidt et al., 2004).

In view of this, the finding in a quartz+mica assemblage of a large crystal of phengite together with seemingly exsolved phlogopite motivated the present investigation. Note that, an exsolving process in a closed system alone cannot account for the coexistence of phengite and phlogopite, and complex metasomatic reactions involving fluids are also to be assumed. The aim of this work is to provide a thermodynamic model that estimates the *P-T* of formation, starting from a detailed crystal-chemical characterisation of the involved micas.

Phengites (*Phe*) are dioctahedral micas (ideal composition: $KAl_{2-x}(Fe, Mg)_x[Si_{3+x}Al_{1-}$

115 $_x]O_{10}(OH)_2$) that usually occur in nature as 2M_1 (more abundant) and 3T polytypes (S.G.
116 $C2/c$ and $P3_112$, respectively). Several 3T structures were refined and reported in literature
117 (Amisano-Canesi at al., 1994; Ivaldi et al., 200; Pavese et al., 1997, 1999, 2000, 2003a;
118 Smyth et al., 2000;Weiss et al., 1993), although special attention must be paid to the
119 reliability of the occupancy factors (Pavese and Diella, 2013). Because of its occurrence in
120 high-pressure metamorphic rocks, the 3T polytype is thought to be more suitable for high P
121 conditions than 2M_1.The 3T polytype presents two independent occupied octahedral-sites
122 (Ferraris et al., 1995; Ferraris and Ivaldi, 2002) while the 2M_1 only shows one. The 3T to
123 2M_1 transition is supposed to take place upon decreasing the P/T ratio (Ivaldi et al., 2001;
124 Sassi et al., 1994). The occurrence of one polytype instead of the other is useful in
125 constraining the pressure-temperature conditions of formation.
126 In the metamorphic dioctahedral micas, the ^{IV}Si content increases with increasing
127 crystallisation pressure. Single crystals of quartz platelets, 100-700 Å thick, were observed,
128 along with talc, in a phengite coming from the UHP Brossasco-Isasca Unit of southern
129 Dora-Maira Massif, Western Italian Alps (Ferraris et al., 2000). Their occurrence was
130 related to an intra-crystalline re-organisation during decompression of the original
131 phengites.
132 Phlogopites (*Phl*) are trioctahedral micas (ideal composition $KMg_3[Al\ Si_3]O_{10}(OH)_2$) that
133 usually crystallise as 1M (S.G. $C2/m$) and rarely as 3T (S.G. $P3_112$) polytypes. Only two
134 phlogopites 3T were refined and reported in literature: the first one comes from Traversella
135 - Western Alps (Gatta et al., 2011) and the second from Kasenyi – Uganda (Schingaro et
136 al., 2013).
137 A miscibility gap between dioctahedral and trioctahedral micas is known. Lester (1946)
138 and Gresen et al. (1971) described exsolutions in micas coming from Mitchell Creek

(Georgia, USA). The quoted authors observed unusual and pyramidal intergrowths of biotite in muscovite. Two instances of transmission electron microscopy investigations on trioctahedral exsolutions in magmatic muscovite $2M_1$ were reported: very small exsolutions (~10nm scale) in muscovite from Lawler Peak granite -Arizona (Ferrow et al., 1990) and ferro-aluminian phlogopitic lamellae (~1mm scale) in muscovite from pegmatite outcropping near Gorduno -Switzerland (Ferraris et al., 2001). Experimental studies in the system K_2O-M^{2+}-Al_2O_3-SiO_2-H_2O±(HF) with M^{2+}=Mg^{2+} or Fe^{2+} at *P*~ 2 kbar and variable *T* (200-700°C) showed a relevant dependence of the solid solution stability on temperature (Monier and Robert, 1986a, 1986b).

Understanding the principles underlying the coexistence of the observed phengite and phlogopite in a quartz dominated (silica oversaturated) mineral assemblage of the Sulu vein, will shed light on the "peculiar" *P-T-X* conditions and evolution of the process involved in their formation.

2. Materials and Methods

2.1. Sample Description

The original specimen is a large, flat, regular flake (about 20 cm ×15 cm × 2 cm) of a seemingly hosting phengite mica, characterised by a homogeneous deep green colour. Optical observations and single crystal X-ray rotation photos were performed on several samples extracted from different regions of the phengite mica. They confirmed an overall homogeneous trigonal symmetry of the phengite mica (Fig. 2).

In some areas of the sample, especially near the margins of the flake, associations of quartz and brown micas were observed (Fig. 3). Their nucleation and growth are clearly

successive to the hosting phengite crystallisation, because of the preserved iso-orientation of the (001) plane in both hosted- and hosting-micas. This suggests the occurrence of exsolving processes, with the contribution from an "external chemical supplier" (most probably ascribable to fluid circulation). Therefore, the term "*quasi*-exsolution" is used hereafter to address a non-isochemical exsolution process. Such *quasi*-exsolved micas have sub-millimetre extension and micrometre thickness; their shape can be euhedral and pyramidal (Lester, 1946. Fig. 2), or irregular (Fig. 3). Several *quasi*-exsolved mica samples were extracted and tested by single crystal X-ray rotation photos. Most of the specimens are trigonal, and only a few present monoclinic symmetry.

2.2 Analytical methods

A fragment of the original mica-matrix sample was grounded to carry out preliminary X-ray powder diffraction characterisations. The measurements were performed by a Huber-Guinier 670 camera, CuKα radiation, scan range $2°<2\theta<70°$ and the diffraction patterns were processed by the GSAS Software Package.

The combination of X-ray powder diffraction, optical observations and chemical composition from micro-analyses, revealed the simultaneous occurrence of a major phengite (hereafter *Phe-3T*) and two minor phlogopite polytypes (*Phl-3T* and *Phl-1M*, for trigonal and monoclinic *quasi*-exsolved phlogopites, respectively). Single crystal specimens were separated for X-ray diffraction, which was performed at room temperature using MoKα radiation by both a Siemens P4 diffractometer, equipped with a point detector (University of Turin), and a Gemini R Ultra X-ray diffractometer, equipped with a Ruby CCD detector (CrisDi Interdepartmental Center for Crystallography, University of Turin). The former was used to measure lattice parameters of the samples under investigation; the latter to record diffraction intensities. Because of the limited crystal thickness, the *quasi*-

exsolved crystals provided a comparatively small number of *hkl*-reflections. Structure refinements have been performed using both SHELXL-97 package (Sheldrick, 1997) and Jana2006 software (Petricek et al., 2014). *Phl-3T* data allowed a structure refinement using isotropic atomic displacement parameters, only. Single crystal X-ray diffraction experimental setup, overall refinement conditions and lattice parameters of each phase are reported in Table S1.

Four fragments from different areas of the original hosting-phengite flake were embedded in epoxy resin and analysed to determine their for chemical composition. Major element compositions were obtained by an ARL-SEMQ electron microprobe analyser (EMPA) equipped with wavelength- and energy-dispersive spectrometers (University of Modena and Reggio Emilia). The following operating conditions were set: 15 kV and 20 nA beam current. Quartz (Si), corundum (Al), periclase (Mg), magnetite (Fe), rhodonite (Mn), grossular (Ca), rutile (Ti), chromium oxide (Cr), vanadinite (V), albite (Na), apatite (P) have been used as standards for the elements in parentheses.

Mössbauer spectroscopic analyses were performed on the *Phe-3T* sample in order to quantify Fe^{2+} and Fe^{3+}. The spectrum was collected at room temperature on about 80 mg of powdered sample (Fig. 4), by a conventional constant acceleration spectrometer, using a rhodium matrix ^{57}Co source, nominal strength 1850 mBq (University of Padua). To reduce the crystal iso-orientation, a ‘‘magic angle’’ setting was used (54° between the incident beam and the sample plain). The hyperfine parameters isomer shift (δ), quadrupole splitting (Δ), full linewidth at half maximum (Γ), were expressed in mms−1 while the relative area (A) in %. The parameters were obtained by means of standard least-squares minimiaation techniques. The spectra were fitted to Lorentzian line shapes with the minimum number of doublets. δ is quoted to α-Fe, using a 4-lines calibration.

The water content was assessed by means of thermogravimetric analyses (TGA). TG analyses were carried out under dynamic nitrogen atmosphere (35 mL min^{-1}) by a Pyris 1 ultra-micro-balance - Perkin Elmer. The sample was heated in the temperature range 30-1000 °C (heating rate 20 °C min^{-1}) and an overall weight loss of 4.5% was observed. A first process, observed between 30 and 180 °C, was responsible for a weight loss of 0.5% and was attributed to the desorption of physisorbed water. From 180°C the sample continuously lost weight up to 980 °C due to a not well defined process which was responsible for a weight loss of 4% and was reasonably attributed to the evolution of structural water.

3. Results

Phe-3T and *quasi*-exsolved *Phl*-phases major element compositions are reported in Table 1, whereas the doublets best fit parameters of Mössbauer patterns are listed in Table S2. On the basis of EMPA and Mössbauer analyses, the chemical formula unit of *Phe-3T* (calculated according to 22 negative charges) is:

$(K_{0.96}Na_{0.02}Ba_{0.01})(Al_{1.35}Mg_{0.40}Fe^{2+}_{0.11}Fe^{3+}_{0.13}Ti_{0.02})_{\Sigma=2.02}[Si_{3.44}Al_{0.56}]O_{10}(OH)_2$.

Quantitative chemical analyses performed on the *Phl-3T* specimens provided the following chemical formula unit:

$(K_{0.78}Na_{0.01})(Mg_{1.48}\ Fe^{2+}_{0.39}Fe^{3+}_{0.45}Al_{0.30}Ti_{0.06})_{\Sigma=2.68}[Si_{2.98}Al_{1.02}]O_{10}((OH)_{1.77}F_{0.23})$.

Comparing the two compositions, *Phl-3T* is consistently richer in Fe and Mg than *Phe-3T*, but the $^{VI}Mg/^{VI}Fe$ ratio in the two phases is similar [$(^{VI}Mg/^{VI}Fe)_{Phe\text{-}3T}$ = 1.70, $(^{VI}Mg/^{VI}Fe)_{Phl\text{-}3T}$ = 1.63].

The analyses on the *quasi*-exsolved monoclinic polytype, *Phl-1M*, provided a chemical

236 composition very close to the trigonal polytype's:

237 $(K_{0.85}Ca_{0.01})(Mg_{1.43} Fe^{2+}_{0.45}Fe^{3+}_{0.54}Al_{0.21}Ti_{0.06})_{\Sigma=2.69} [Si_{2.88}Al_{1.12}]O_{10}((OH)_{1.99}F_{0.01})$.

238 Changes of composition from *Phe-3T* to its phlogopite *quasi*-exsolved products were
239 measured along radial directions departing from the separation edge (Fig. 5). A shell with
240 variable width (~300-500 μm) and zoned composition was found: approaching the *quasi*-
241 exsolved phases, Si and Al decrease, while Fe and Mg increase (Table 1; Fig.5). Midway
242 along the transition region from phengite to phlogopite, the following approximated
243 composition occurs:

244 $(K_{0.89}Na_{0.02}) (Al_{1.24}Fe_{0.52}Mg_{0.54}Ti_{0.02})_{\Sigma=2.32} [Si_{3.16}Al_{0.84}] O_{10}(OH)_2$.

245 The compositions of *Phl-1M* and *Phl-3T* correspond in micas' nomenclature (Rieder et al.,
246 1998) to "ferrian aluminian phlogopite"; abbreviated to "phlogopite" in the rest of the
247 study.

248

249 *3.1 Phe-3T and Phl-polytypes*

250

251 *3.1.1 Phe-3T*

252 The average distances <T1-O> and <T2-O> are equal (1.631(1) Å; Tables S3 and S4) and
253 in agreement with literature values. The ditrigonal rotation (Table S5) of the tetrahedral
254 sheet (~4.48°) is in keeping with a HP regime (Curetti et al., 2008).

255 The average distances <M2-O> and <M3-O> are meaningfully different (1.958(1) Å and
256 1.972(1) Å, respectively) and indicate a partial octahedral ordering of large cations in M3,
257 although the refined number of electrons (14.3(2) *e* and 14.7(2) *e* in M2 and M3,
258 respectively; Table S3) cannot confirm this inference from bond-lengths.

259 Mössbauer spectroscopy suggests partial octahedral ordering of iron: (i) Fe^{3+} absorption is

modelled by only one doublet, which suggest that the trivalent iron is completely ordered in one octahedron (0.13 Fe^{3+} a.p.f.u.); (ii) Fe^{2+} absorption is fitted by two doublets, each corresponding to one site (0.05 and 0.06 Fe^{2+} a.p.f.u.). Several Mössbauer analyses on dioctahedral micas $2M_1$ were reported in literature (Aldrige et al., 1987; Finch et al., 1982; Goodman, 1976; Shabani et al., 1998). The patterns usually show two different doublets for Fe^{2+}, even if they are expected to have only one occupied symmetry independent octahedral site. To explain the unexpected second doublet (very weak and corresponding to 0.03-0.04 Fe^{2+} a.p.f.u., at most) the quoted authors assumed a partial occupancy of the M1–*trans* site. The 3*T* polytype has two independent octahedral sites (M2 and M3) and the two Fe^{2+} doublets can be assigned without resorting to the M1 empty site (Merli et al., 2009; Pavese et al., 2000; Pavese et al., 2001;). In fact, partial and very low M1 occupancy is suggested by both chemical analyses (octahedral cations sum = 2.02 a.p.f.u.) and structural refinement (0.86 *e* in the Fourier difference, 0.3(1) *e* refined), though the electron content corresponding to each Mössbauer doublet is too high in comparison with the M1 refined occupancy (0.05 a.p.f.u. corresponding to about 1.3 *e*). Mössbauer spectroscopy is not able to univocally associate iron doublets to specific sites, however its combination with structure refinements allows one to infer a partially ordered distribution of Fe, Al and Mg. The M1 octahedral site is almost completely empty. The H atom position was determined by the Fourier Difference and refined; the O-H distance is 0.80(4) Å and the angle between O-H bond and (0 0 1) plane is ~6.55°.

3.1.2 Phl-3T

Several crystals of phlogopite *3T* were sampled from the hosting phengite *Phe-3T*, but only a few were suitable for measurements and structure refinements. Such specimens are about

200-400 μm in length and width, and very thin (<50 μm). A modest number of reflections were measured for *Phl-3T* and the structural refined parameters show large uncertainties, as shown in the figure of merit reported in Table 1, i.e. $R[|F_o| > 4\sigma(|F_o|)]=8.50\%$. Therefore structure constraints were introduced in the refinement strategy. The atomic displacement parameters have been constrained as follows: $U_{iso}(M1) = U_{iso}(M2) = U_{iso}(M3)$, $U_{iso}(T1) = U_{iso}(T2)$, $U_{iso}(O1) = U_{iso}(O2) = U_{iso}(O3) = U_{iso}(O4) = U_{iso}(O5) = U_{iso}(O6)$ (Table 4). Conversely, the fractional coordinate distances were refined without any constraint, and the cation-anion distances were determined accordingly.

The structural results can be compared with those of the trigonal phlogopite samples from Traversella (*Phl*-TR) and from Uganda (*Phl*-UG). In *Phl*-TR <M1-O> is 2.079 Å, and 2.072(6) Å in *Phl*-UG. In both samples, <M1-O>s are not significantly different from <M2-O> and <M3-O>. Conversely, the trigonal phlogopite sample investigated here, exhibits <M1-O> of 2.245(3) Å, some 10% longer than <M2-O> = 1.991 (8) Å and <M3-O> = 2.052(8) Å (Table S4).

The occupancy factors of Fe-Al-Mg-Si in the tetrahedral and octahedral sites were not refined and the cations were arranged according to a completely disordered distribution. Only the number of electrons in the interlayer site was refined, as 16.9(2) *e*.

Comparing the distortion parameters (Table S5) with those reported for *Phl*-TR/UG, *Phl-3T* is more strained. Such an aspect is more marked in *Phl*-UG. The major distortions are not related to bond lengths, but mainly to angular values, thus suggesting that the structure strain is probably due to the *Phl-3T*'s growth process, which took place as a progressive substitution of the pre-existing framework of *Phe-3T*.

307 *3.1.3 Phl-1M*

308 Only a few specimens of monoclinic *quasi*-exsolved phase were found in the hosting
309 phengite. Using the largest one we performed single crystal X-ray diffraction experiments
310 with a satisfactory number of reflections. The structure refinement in the S.G. *C*2/*m*
311 converged to R ~ 4.78% (Table S3).

312 The cell parameters (a = 5.3195(13) Å, b = 9.2117(12) Å, c = 10.210(3) Å, β = 100.04(2)°,
313 V = 492.7(2) Å^3; Table S4) are in excellent agreement with the ones of *Phl-3T* (a =
314 5.318(1) Å, c = 30.21(2) Å; $c_{(1M)} \times \text{sen}\,\beta_{(1M)}$ = 30.16 Å).

315 Average bond distances $\langle T\text{-}O\rangle_{1M}$ = 1.652(1) Å, $\langle M\text{-}O\rangle_{1M}$ = 2.074(1) Å and $\langle I\text{-}O\rangle_{1M}$ =
316 3.159(1) Å are very similar to the corresponding values in *Phl-3T* sample (Tables S3 and
317 S4). The two M-O distances are meaningfully different from one another (<M1-O> =
318 2.088(1); <M2-O> = 2.061(1) Å), but the refined electron content (14.17(14) and
319 14.18(12) *e* for M1 and M2, respectively) does not indicate any cation order.

320 *Phl-1M* yields bond-lengths, bond-angles and distortion parameters (α=8.00°, Δz=0.01Å;
321 Δ_{TM} = 0.44Å, BLD_{M1} = 0.76%, BLD_{M2} = 0.80%, J_{M1} = 0.00° and J_{M2} = 0.88°; Table S5) in
322 agreement with those reported in literature on phlogopite 1*M* (Brigatti and Guggenheim,
323 2002).

324

325 **4. Discussion**

326

327 *4.1 Mass balance calculation*

328 The rock containing the studied micas and quartz is a thick metamorphic vein, similar to
329 those commonly observed in the Sulu UHP terrane. A not-weighted mass balance
330 calculation (Wright and Doherty, 1970) was used to provide the best match between the

sampled mineralogical assemblage and fluid alkali-alumino-silicate components that mirror the bulk rock averaged compositions of the Sulu-vein (*ASV*), reduced to an anhydrous major oxides system (Table 2):

x_1 *Phe-3T* + x_2 quartz + x_3 *Phl-3T* + x_4 *Phl-1M* + x_5 K-feldspar = 1 *ASV* (1)

where x_i represents the *i*-phase proportion. The solution is (least square residuum, r^2=0.8):

0.574 *Phe-3T* + 0.488 quartz + (-0.049) *Phl-3T* + (-0.002) *Phl-1M* + (-0.001) K-feldspar =1 *ASV* (2)

Eq.(2) demonstrates that *ASV* accounts for a phengite-quartz based rock and the occurrence of phlogopite micas can be explained as an effect of disproportion in combination with a supply of elements, *i.e*. Mg, Al and K, most probably solute components of alkali-alumino-silicate aqueous solutions at high pressure rock-fluid interactions.

Such results agree with the observed petrographic characteristics of the vein fragment from which the studied micas were extracted: (1) phengite and quartz are comparably proportioned in the rock; (2) the negative phase proportion coefficients suggest that phlogopites are *per force* scarce and only occur as *quasi*-exsolved phases, in combination with an elemental supply from alkali-alumino-silicate high pressure fluids; (3) K-feldspar is modally absent in the fragment, as the negligible resulting negative proportion (*i.e*. -0.001) suggests.

4.2 *P-T-X Equilibrium phases in an open system*

The coexistence of *Phe-3T, Phl-3T* and *Phl-1M* micas cannot be reduced to bare exsolving reactions in a closed system and a contribution from an "external chemical supplier", *i.e*. a "*reservoir*", has to be taken into account (eq.(2)). Therefore, the reactions were modelled

in terms of an open system. Following Merli et al. (2017), the "reservoir" is now seen as a matter exchanger, whose composition, addressed by *Res*(A/B), encompasses all the potential solids and fluids taking part in the petrogenetic reactions, but micas and quartz. A/B are used to indicate a specific chemical condition of the reservoir. In this case, we modelled the reaction process from phengite to phlogopite with the following transformation:

phengite + *Res*(A) = phlogopite +λ quartz + *Res*(B) (3)

where λ is related to the amount of quartz exsolved from the reacting phengite, *i.e.* λ≈0.46. The equilibrium conditions of the assemblage require that

$$\Delta G = G(\text{phengite}) + G[Res(\text{A})] - G(\text{phlogopite}) - G[Res(\text{B})] - \lambda\, G(\text{quartz}) =$$

$$G(\text{phengite}) - G(\text{phlogopite}) - \lambda\, G(\text{quartz}) + \{G[Res(\text{A})] - G[Res(\text{B})]\} =$$

$$G(\text{phengite}) - G(\text{phlogopite}) - \lambda\ G(\text{quartz}) + \delta G[Res] = 0\ , \qquad (4)$$

where G is the molar Gibbs energy of a given phase, *i.e.* its chemical potential, and $\delta G[Res]$ is the molar Gibbs energy difference between *Res*(A) and *Res*(B). Phengite and phlogopite refer to *Phe-3T* and *Phl-3T*, respectively.

The Gibbs energy of a phase at given *P*-*T* conditions can be determined by two distinct integrations, one along an isobar at P_0 and the other along an isotherm at *T*, *i.e.*

$$G(P,T) = G(P_0,T_0) - \int_{T_0}^{T} S\,(P_0,T')dT' + \int_{P_0}^{P} V(P',T)dP' \qquad (5)$$

where P_0 and T_0 are in general reference pressure and temperature (for explicit calculations refer to Pavese and Diella, 2007), here corresponding to room pressure and temperature. Equation (5) can be written as

$$\Delta G(P,T) = \Delta G(P_0,T_0) + \Delta I_{T-T_0} + \Delta I_{T-T_0,\text{config}} + \Delta I_{P-P_0}. \qquad (6)$$

where $\Delta G(P_0,T_0)$ is the formation energy with respect to the standard state of the constituent oxides. ΔI_{P-P_0} is due to the solid phases of eq. (4), *i.e.* micas and quartz, and it

379 can be determined by means of the equations of state of the involved minerals. We used a
380 third order Birch-Murnaghan *P-V-T* relationship and thermo-elastic parameters from
381 Amisano-Canesi et al. (1994); Angel et al. (1997); Chon et al. (2003, 2006); Comodi et
382 al. (1999); Curetti et al. (2006); Gatta et al. (2009, 2011), Gemmi et al. (2008). Hazen
383 and Finger (1978); Russell and Guggenheim (1999); Takeda and Morosin (1975) and
384 Ventruti et al. (2009).
385 $\Delta G(P_0, T_0)$ + I_{T-T_0} were estimated by the reaction:
386 $\frac{1}{2}$ muscovite + $\frac{1}{4}$ celadonite + $\frac{1}{4}$ Fe − celadonite + 1.75 periclase + 0.75 wüstite =
387 $\frac{2}{3}$phlogopite + $\frac{1}{3}$ annite + $\frac{1}{2}$corundum + $\frac{1}{2}$quartz
388 taking the Gibbs energy of formation and heat capacity at constant pressure from Holland
389 and Powell (1998). The $\Delta G(P_0, T_0)$ + I_{T-T_0} is modest and weakly dependent on *T* in the
390 investigated 770-1200 K thermal range. In was therefore approximated by a constant as
391 large as 13 kJ/mol. However, taking into account the high degree of approximation, we
392 assumed a confidence range from 10 to 15 kJ/mol, and explored its limits. Lastly,
393 $\Delta I_{T-T_0,\text{config}}$ is due to the configuration contribution to entropy, S_{config}, which is calculated
394 as follows:
395 $$S_{\text{config}} = -\text{R}\sum_{j=1}^{sites}\sum_{\alpha=1}^{chemical\ species} p_{j,\alpha}\ln\left(p_{j,\alpha}\right)$$
396 where R is the universal gas constant and $p_{j,\alpha}$ is the occupancy factor of the α–species at
397 the j^{th}-sites. In figure 6 we display the *P-T loci* (GPa and °C) of equilibrium for reaction
398 (4), with $\Delta G(P_0, T_0)$ + I_{T-T_0} equal to 10 and 15 kJ/mol, respectively.
399 The intersection between the equilibrium *P-T locus* and the supposed *P-T* metamorphic
400 path of OH-rich quartzite from Sulu UHP terrane from Frezzotti et al. (2007) occurs at $P \approx$
401 2.4±0.2 GPa and $T \approx$ 700 °C. Such a result is consistent with the observation of Hermann

and Green (2001), if the phengite existence curve of the quoted authors is extrapolated to 700 °C.

On the basis of petrological data, stable isotope geothermometry and theoretical phase relationships of quartzites from Sulu terrane, the UHP fluids composition estimated by Frezzotti et al. (2007) is an intermediate alkali-alumino-silicate aqueous solutions (H_2O ~50 wt %), that constrains the metamorphic peak at $P \sim 3.5$ PGa and $T \sim 780$ °C .

The obvious compositional similarity between the quartzites investigated by Frezzotti et al. (2007) and the Sulu vein of this study allowed us to state that the calculated P-T conditions for phlogopite growth in a SiO_2 oversaturated system indicate at a region that reflects early stages of exhumation, close to the metamorphic peak (Fig. 6).

5. Conclusions

The main purpose of this work was to study the rare coexistence of dioctahedral mica and trioctahedral *quasi*-exsolutions observed in a thick quartz+phengite metamorphic vein found in the northern part of Sulu UHP metamorphic terrane, of Donghai County (eastern China).

The process leading to such an assemblage is described as a "*quasi*-exsolution" process and it is constituted by non-isochemical exsolution . The composition change is due to an external supplier.

The reaction process from phengite to phlogopite favours /requires the exsolution of quartz. Because of the trigonal structure provided from phengite, the *quasi*-exsolved phlogopite crystallised as *3T*-polytype, which is unusual for trioctahedral micas.

Mass balance calculations suggest that the phengite-quartz based rock and the occurrence of phlogopite micas can be explained as an effect of disproportion in combination with a

supply of elements, *i.e*. Mg, Al and K, from alkali-alumino-silicate high pressure fluids, that mirror the bulk Sulu vein composition.

The calculated equilibrium *P-T locus* of phengite-phlogopite-quartz reaction intersects the *P-T* metamorphic path at $P \approx 2.4 \pm 0.2$ GPa and $T \approx 700$ °C, indicating an early stage of exhumation, close to the metamorphic peak of the Sulu UHP terrane.

Acknowledgements

The studied phengite was collected in 2000, during a field expedition in the Sulu orogene, organised by Prof. Xu Shutong in the framework of a Chinese-Italian cooperation project (R.C The authors thank the Editor Marco Scmbelluri, Patrizia Fumagalli and anonymous reviewer for their positive comments. The authors would like to thank the "Compagnia di San Paolo" of Turin, Italy, for supporting the TGA measurements. L.N would like to thank the Department of Chemical Science, University of Padua, for allowing the free use of Mössbauer spectrometer.

The paper benefited of the English language editing provided by Barbara Galassi (Brighton, U.K)

Part of this research was supported by MIUR-2015 20158A9CBM Grant (C.B).

References

Aldridge, L.P., Finch, J, Gainsford, A.R., Tennant, W.C., Childs, C.W., 1987. Electric-field gradient in muscovites. American Mineralogist 72, 528-536.

Amisano-Canesi, A., Chiari, G., Ferraris, G., Ivaldi, G., Soboleva, S.V., 1994. Muscovite- and phengite-3T: crystal structure and conditions of formation. European Journal of Mineralogy 6, 489-496.

452 Angel, R.J., Allan, D.R., Miletich, R., Finger, L.W., 1997. The use of quartz as an internal
453 pressure standard in high pressure crystallography. Journal of Applied
454 Crystallography 30, 461-466.
455 Brigatti, F., Guggenheim, S., 2002. Mica crystal chemistry and the influence of pressure,
456 temperature, and solid solution on atomistic models. Reviews in Mineralogy and
457 Geochemistry 46, 1-97.
458 Castelli, D., Rolfo, F., Compagnoni, R., Xu, S.T., 1998. Metamorphic veins with kyanite,
459 zoisite and quartz in the Zhu-Jia-Chong eclogite, Dabie Shan, China. Island Arc
460 7(1-2), 159-173.
461 Chon C-M, Kim SA, Moon H-S, 2003. Crystal structure of biotite at high temperatures and
462 of heat-treated biotite using neutron powder diffraction. Clays and Clay Minerals
463 51, 519–528.
464 Chon, C.-M., Lee, C.-K., Song, Y., Kim, S.-A., 2006. Structural changes and oxidation of
465 ferroan phlogopite with increasing temperature: in situ neutron powder diffraction
466 and Fourier transform infrared spectroscopy, Physics and Chemistry of Minerals
467 33(5), 289-299.
468 Comodi, P., Zanazzi, P.F., Weiss, Z., Rieder, M., Drábek, M., 1999. "Cs-ferri-tetra-
469 annite": high-pressure and high-temperature behavior of a potential nuclear waste
470 disposal phase. American Mineralogist 84, 325-332.
471 Compagnoni, R., Engi, M., Regis, D., 2014. Val d'Aosta section of the Sesia Zone: multi-
472 stage H*P* metamorphism and assembly of a rifted continental margin**.** 10th Int.
473 Eclogite Conf., Syn-Conference Excursion, 5 September 2013, GFT – Geological
474 Field Trips, 6 (1.2), 1-44. ISSN: 2038-4947. (DOI 10.3301/GFT.2014.02)
475 http://www.isprambiente.gov.it/it/pubblicazioni/periodici-tecnici/geological-field-

trips/valle-daosta-section-of-the-sesia-zone.

Cong, B.-L., Wang, Q.C., Zhai, M., Zhang, R.Y., Zhao, Z.Y., Ye, K., 1994. Ultrahigh-pressure metamorphic rocks in the Dabishan–Sulu Region of China. Island Arc 3, 135–150.

Curetti, N., Levy, D., Pavese, A., Ivaldi, G., 2006. Elastic properties and stability of coexisting 3T and 2M1 phengite polytypes. Physics and Chemistry of Minerals 32(10), 670 – 678.

Curetti, N., Ferraris, G., Ivaldi, G., 2008. Correlation between crystallization pressure and structural parameters of phengites. American Mineralogist 93, 451-455.

Deng, L.-P., Liu, Y.-C., Gu, X.-F., Groppo, C., Rolfo, F., 2017. Partial melting of ultrahigh-pressure metamorphic rocks at convergent continental margins: Evidences, melt compositions and physical effects, Geoscience Frontiers. http://dx.doi.org/10.1016/j.gsf.2017.08.002

Desmons, J., O'Neill, J.R., 1978. Oxygen and hydrogen isotope compositions of eclogites and associated rocks from the eastern Sesia Zone (Western Alps, Italy). Contributions to Mineralogy and Petrology 67, 79-85.

Droop, G.T.R., Lombardo, B., Pognante, U., 1990. Formation and distribution of eclogite facies rocks in the Alps. In: D.A. Carswell, (Ed.) Eclogite Facies Rocks. Glasgow, Blackie, 225-259.

Ferrando, S., Frezzotti, M.L., Dallai, L., Compagnoni, R., 2005. Fluid-rock interaction in UHP phengite-kyanite-epidote eclogite from the Sulu Orogen, Eastern China. International Geology Review 47, 750-774.

Ferraris, G., Ivaldi, G., 2002. Micas: crystal chemistry and metamorphic petrology. Reviews in Mineralogy and Geochemistry 46, 117-153.

Ferraris, G., Ivaldi, G., Nespolo, M., Takeda, H., 1995. On the stability of dioctahedral

micas. Terra Abstract (suppl. N.1 Terra Nova) 7, 289.

Ferraris, C., Chopin, C., Wessicken, R., 2000. Nano- to micro-scale decompression products in ultrahigh-pressure phengite: HRTEM and AEM study, and some petrological implications. American Mineralogist 85, 1195-1201.

Ferraris, C., Grobety, B., Wessicken, R., 2001. Phlogopite exsolution within muscovite: a first evidence for a higher-temperature re-equilibration, studied by HRTEM and AEM techniques. European Journal of Mineralogy 13, 15-26.

Ferrow, E.A., London, D., Goodman, K.S., Veblen, D.R., 1990. Sheet silicates of the Lawler Peak granite, Arizona: chemistry, structural variations, and exsolution. Contributions to Mineralogy and Petrology 105, 491-501.

Finch, J., Gainsford, A.R., Tennant, W.C., 1982. Polarized optical absorption and ^{57}Fe Mössbauer study of pegmatitic muscovite. American Mineralogist 67, 59-68.

Frank, W., Hock, V., Miller, C., 1986. Metamorphic and tectonic history of the Central Tauern Window. In: H.W. Flugel, P. Faupl (Eds.), Geodynamics of the Eastern Alps, Deuticke, Vienna, 34-54.

Frezzotti, M.L., Ferrando, S., Dallai, L., Compagnoni, R., 2007. Intermediate alkali-alumino-silicate aqueous solutions released by deeply-subducted continental crust: fluid evolution in UHP OH-rich topaz-kyanite-quartzites from Donghai County (Sulu, China). Journal of Petrology 48, 1219-1241.

Gatta, G.D., Rotiroti, N., Pavese, A., Lotti, P., Curetti, N., 2009. Structural evolution of a 3T phengite mica up to 10 GPa: an in-situ single-crystal X-ray diffraction study. Zeitschrift für Kristallographie 224, 302-310.

Gatta, G.D., Merlini, M., Rotiroti, N., Curetti, N., Pavese, A., 2011. On the crystal chemistry and elastic behavior of a phlogopite 3T. Physics and Chemistry of

525 Minerals 38, 655-664.
526 Gemmi, M., Merlini, M., Pavese, A., Curetti, N., 2008. Thermal expansion and
527 dehydroxylation of phengite micas. Physics and Chemistry of Minerals 35(7), 367-
528 379.
529 Goodman, B.A., 1976. The Mössbauer spectrum of a ferrian muscovite and its implications
530 in the assignment of sites in dioctahedral micas. Mineralogical Magazine 40, 513-
531 517.
532 Gresens, R.L., Stensrud, H.L., 1971. Chemical, optical, and X-ray analysis of an unusual
533 muscovite-biotite intergrowth. Lithos 4, 63-69.
534 Hazen, R.M., Finger, L.W., 1978. The crystal structures and compressibilities of layer
535 minerals at high pressure. II Phlogopite and Chlorite. American Mineralogist 63,
536 293-296.
537 Hermann, J., Green, D.H., 2001. Experimental constraints on high pressure melting in
538 subducted crust. Earth and Planetary Science Letters 188, 149-168.
539 Hermann, J., Rubatto, D., 2009. Accessory phase control on the trace element signature of
540 sediment melts in subduction zones. Chemical Geology 265, 512–526.
541 Hirajima, T., Nakamura, D., 2003. The Dabie Shan– Sulu orogeny. In: D.A., Carswell and
542 R., Compagnoni (Eds.), Ultrahigh-pressure metamorphism. E.M.U. Notes in
543 Mineralogy 5, 105–144. Eötvös University Press, Budapest.
544 Holland, T.J.B., Powell, R., 1998. An internally consistent thermodynamic data set for
545 phases of petrological interest. Journal of Metamorphic Geology 16, 309-343.
546 Ivaldi, G., Ferraris, G., Curetti, N., Compagnoni, R., 2001. Coexisting 3T and 2M1
547 polytypes of phengite from Cima Pal (Val Savenca, western Alps): Chemical and
548 polytypic zoning and structural characterisation. European Journal of Mineralogy

549 13, 1025-1034.
550 Lester, J.G., 1946. Inclusions in muscovite from Mitchell Creek Mine, Upson Country,
551 Georgia. American Mineralogist 31, 77-81.
552 Li X.-P., Li Y.-L., Shu G.-M., 2005. Breakdown of lawsonite subsequent to peak UHP
553 metamorphism in the Dabie terrane and its implication for fluid activity. Chinese
554 Science Bulletin 50(13), 1366-1372.
555 Liu, Y.-C., Deng, L., Gu, X., Groppo, C., Rolfo, F., 2015. Application of Ti-in-zircon and
556 Zr-in-rutile thermometers to constrain high-temperature metamorphism in eclogites
557 from the Dabie orogen, central China. Gondwana Research 27, 410-423.
558 Massonne, H.-J., Szpurka, Z., 1997. Thermodynamic properties of white micas on the basis
559 of high-pressure experiments in the systems K_2O-MgO-Al_2O_3-SiO_2-H_2O and K_2O-
560 FeO-Al_2O_3-SiO_2-H_2O. Lithos 41, 229-250.
561 Mattinson C.G., Zhang R-Y., Tsujimori T., Liou J.G., 2004. Epidote-rich talc-kyanite-
562 phengite eclogites, Sulu terrane, eastern China: P-T-fO2 estimates and the
563 significance of the epidote-talc assemblage in eclogite. American Mineralogist
564 89(11-12), 1772-1783.
565 Merli, M., Pavese, A., Curetti, N., 2009. Maximum entropy method: an unconventional
566 approach to explore observables related to the electron density in phengites. Physics
567 and Chemistry of Minerals 36, 19-28.
568 Merli, M., Bonadiman, C., Diella, V., Sciascia, L., Pavese, A., 2017. Fe-periclase reactivity
569 at Earth's lower mantle conditions: Ab-initio geochemical modelling. Geochimica
570 et Cosmochimica Acta 214, 14-29.
571 Monier, G., Robert, J.L., 1986a. Muscovite solid solutions in the system K_2O-MgO-FeO-
572 Al_2O_3-SiO_2-H_2O: an experimental study at 2 kbar P_{H2O} and comparison with natural

573 Li-free white micas. Mineralogical Magazine 50, 257-266.
574 Monier, G., Robert, J.L., 1986b. Evolution of the miscibility gap between muscovite and
575 biotite solid solutions with increasing lithium content: an experimental study in the
576 system K_2O-Li_2O-MgO-FeO-Al_2O_3-SiO_2-H_2O-HF at 600°C, 2 kbar P_{H2O}:
577 comparison with natural lithium micas. Mineralogical Magazine 50, 641-651.
578 Pavese, A., Diella, V., 2007. Uncertainties on elastic parameters and occupancy factors:
579 how do they affect the accuracy of the calculated Gibbs energy of minerals at (P,T)
580 conditions? The case of 3T- versus $2M_1$ phengite. Physics and Chemistry of
581 Minerals 34(9), 637-645.
582 Pavese, A., Diella, V. 2013. How stacking disorder can conceal the actual structure of
583 micas: the case of phengites. DOI:10.1007/s00269-013-0568-6. Physics and
584 Chemistry of Minerals 40, 375-386.
585 Pavese., A., Ferraris, G., Pischedda, V., Ibberson, R., 1997. Cation Site ordering in
586 phengite 3T from Dora Maira massif (western Alps): a variable-temperature
587 neutron powder diffraction study. European Journal of Mineralogy 9, 1183-1190.
588 Pavese, A., Ferraris, G., Pischedda, V., Mezouar, M., 1999. Synchrotron powder
589 diffraction study of phengite 3T from Dora Maira massif: P-V-T equation of state
590 and petrological consequences. Physics and Chemistry of Minerals 26, 460-467.
591 Pavese, A., Ferraris, G., Pischedda, V., Radaelli, P., 2000. Further study of cation ordering
592 in phengite 3T by neutron powder diffraction. Mineralogical Magazine 64, 11-18.

593 Pavese, A., Ferraris, G., Pischedda, V., Fauth, F., 2001. M1-site occupancy in 3T and
594 $2M_1$ phengites by low temperature neutron powder diffraction: Reality or artefact?
595 European Journal of Mineralogy 13, 1071-1078.
596 Pavese, A., Curetti, N., Ferraris, G., Ivaldi, G., Russo, U., Ibberson, R., 2003a.
597 Deprotonation and order-disorder reactions as a function of temperature in a
598 phengite 3T (Cima Pal, western Alps) by neutron diffraction and Mössbauer
599 spectroscopy. European Journal of Mineralogy 15, 357-363.
600 Pavese, A., Levy, D., Curetti, N., Diella, V., Sani, A., 2003b. Equation of state and
601 compressibility of phlogopite by in-situ high pressure X-ray diffraction experiment.
602 European Journal of Mineralogy 15, 455-463.
603 Pavese, A., Curetti, N., Diella, V., Levy, D., Dapiaggi, M., Russo, U., 2007. *P-V* and *T-V*
604 Equations of State of natural biotite: an *in-situ* high pressure and high temperature
605 powder diffraction study, combined with Mössbauer spectroscopy. American
606 Mineralogist 92(7), 1158-1164.
607 Petricek, V., Dusek, M., Palatinus, L., 2014. Crystallographic Computing System
608 JANA2006: General features. Zeitschrift für Kristallographie 229(5), 345-352.
609 Poli, S., Fumagalli P., 2003. Mineral assemblages in ultrahigh pressure metamorphism: A
610 review of experimentally determined phase diagrams. In: D.A. Carswell and R.
611 Compagnoni (Eds.) Ultrahigh-pressure metamorphism. E.M.U. Notes in
612 Mineralogy 5, 307-340. Eötvös University Press, Budapest.
613 Rieder, M., Cavazzini, G., D'Yakonov, Yu.S., Frank-Kamenetskii, V.A., Gottardi, G.,
614 Guggenhein, S., Koval, P.V., Müller, G., Neiva, A.M.R., Radoslovich, E.W.,
615 Robert, J.L., Sassi F.P., Takeda, H., Weiss Z., Wones, D.R., 1998. Nomenclature of
616 the micas. The Canadian Mineralogist 36, 905-912.

617 Geological Society of America, 1991: Rock color chart with genuine Munsell^{R} color chips.
618 Boulder, Colo Ed.
619 Russell, R.L., Guggenheim, S., 1999. Crystal structures of near-end-member phlogopite at
620 high temperatures and heat-treated Fe-rich phlogopite: The influence of the O, OH,
621 F site. The Canadian Mineralogist 37, 711-720.
622 Sassi, F.P., Guidotti, C., Rieder, M., De Pieri, R., 1994. On the occurrence of metamorphic
623 2M1 phengites: some thoughts on polytypism and crystallization condition of 3T
624 phengites. European Journal of Mineralogy 6, 151-160.
625 Schingaro, E., Lacalamita, M., Scordari, F., Mesto, E., 2013. 3T-phlogopite from Kasenyi
626 kamafugite (SW Uganda): EPMA, XPS, FTIR and SCXRD study. American
627 Mineralogist 98, 709-717.
628 Schmidt, M.W., Poli, S., 1998. Experimentally based water budgets for dehydrating slabs
629 and consequences for arc magma generation. Earth and Planetary Science Letters
630 163, 361-379.
631 Schmidt, M. W., Vielzeuf, D., Auzanneau, E., 2004. Melting and dissolution of subducting
632 crust at high pressures: the key role of white mica. Earth and Planetary Science
633 Letters 228, 65-84.
634 Shabani, A.A.T., Rancourt, D.G., Lalonde, A.E., 1998. Determination of cis and trans
635 Fe2+ populations in 2M(1) muscovite by Mossbauer spectroscopy. Hyperfine
636 Interactions, 117, 117-129.
637 Sheldrick, G.M., 1997. SHELXL-97, Program for the Refinement of Crystal Structure;
638 University of Göttingen, Germany.
639 Smyth, J.R., Jacobsen, S.D., Swope, R.J., Angel, R.J., Arlt, T., Domanik, K., Holloway,
640 J.R., 2000. Crystal structures and compressibilities of synthetic $2M_1$ and 3T

641 phengite micas. European Journal of Mineralogy 12(5), 955-963.
642 Takeda, H., Morosin, B., 1975. Comparison of observed and predicted structural
643 parameters of mica at high temperature. Acta Crystallographica B31, 2444-2452.
644 Thomsen, T.B., Schmidt, M.W., 2008. The Biotite to Phengite Reaction and Mica-
645 dominated Melting in Fluid+Carbonate-saturated Pelites at High Pressures. Journal
646 of Petrology 49, 1889-1914.
647 Tutti, F., Dubrovinsky, LS., Nygren, M., 2000. High-temperature study and thermal
648 expansion of phlogopite. Physics and Chemistry of Minerals 27(9), 599-603.
649 Ventruti, G., Levy, D., Pavese, A., Scordari, F., Suard, E., 2009. High-temperature
650 treatment, hydrogen behaviour and cation partitioning of a Fe-Ti bearing volcanic
651 phlogopite by in situ neutron powder diffraction and FTIR spectroscopy. European
652 Journal of Mineralogy 21(2), 385-396.
653 Weiss, Z., Rieder, M., Smrcok, L., Petricek, V., Bailey, S.W., 1993. Refinement of the
654 crystal structures of two “protolithionites”. European Journal of Mineralogy 5,
655 493-502.
656 Wright, T.L., Doherty, P.C., 1970. A linear programming and least-squares computer
657 method for solving petrologic mixing problems. Geological Society of America
658 Bulletin 81, 1995–2008.
659 Xu, H.J., Ye, K., Zhang, J.F., 2012. Temperature of prograde metamorphism,
660 decompressional partial melting and subsequent melt fractional crystallization in
661 the Weihai migmatitic gneisses, Sulu UHP terrane: constraints from Ti-in-zircon
662 thermometer. Journal of Earth Sciences 23, 813–827.
663 Zanazzi, P.F. and Pavese, A., 2002. Behavior of micas at high pressure and high
664 temperature. Reviews in Mineralogy and Geochemistry 46, 98-116.

665 Zhang, R. Y., Hirajima, T., Banno, S., Cong, B., Liou, J. G., 1995. Petrology of ultrahigh-
666 pressure rocks from the southern Sulu region, eastern China. Journal of
667 Metamorphic Geology 13, 659–675.
668 Zhang, R.Y., Yang, J.S., Wooden, J.L., Liou, J.G., Li, T.F., 2005. U–Pb SHRIMP
669 geochronology of zircon in garnet peridotite from Sulu UHP terrane, China:
670 implications for mantle metasomatism and subduction-zone UHP metamorphism.
671 Earth and Planetary Science Letters 237, 729–743.
672 Zhang, Z.M., Xiao, Y.L., Liu, F., Liou, J.; Hoefs, J., 2005. Petrogenesis of UHP
673 metamorphic rocks from Qinglongshan, Southern Sulu, East-Central China. Lithos
674 81, 189-207
675 Zheng, Y., Zhou, J.-B., Wu, Y.-B., Xie, Z., 2005. Low-grade metamorphic rocks in the
676 Dabie–Sulu orogenic belt: a passive-margin accretionary wedge deformed during
677 continent subduction. International Geology Review 47, 851–871.
678

Figure 1. Simplified geologic sketch map of the Sulu orogen showing major tectonic units. YQWF, Yantai-Qingdao-Wulian fault White circles mark the location of labelled towns (from Mattinson et al., 2004 and Zhang et al., 2005, modified); The phengite+quartz metamorphic vein was excavated at Qinglongshan (evidenced in the map), in the Donghai County.

Figure 2. Optical micrograph (plane polarised light) of Fe-phlogopite *quasi*-exsolution (brown colour) developed in pyramidal form (its thickness increases toward the centre), with several evident growth stages.

Figure 3. Optical micrographs of mica *quasi*-exsolutions and quartz crystals in trigonal phengite observed under plane polarised (a) light and crossed polarised (b) lights, respectively. The *quasi*-exsolution is apparent in (a) (darker portions) while the mica-quartz reaction is amplified in (b) (white portions).

Figure 4. Mössbauer spectrum collected on *Phe-3T* sample. The peaks are fitted with three doublets and they indicate that 57(1)% of the total Fe is trivalent, 43(1)% bivalent (parameters in Table S1).

Figure 5. Changes of chemical composition from *Phe-3T* to *Phl-3T*; (a) schematic representation of the analysed sample and location of the analysis points. (b) The histogram reports the variation by weight % of the principal oxides; approaching the *quasi*-exsolved phases, Si and Al decrease, while Fe and Mg increase.

703

704 **Figure 6**. Pressure-temperature loci of equilibrium for the phengite-phlogopite-quartz
705 reaction (eq. 2). The cases of $\Delta G(P_0, T_0)$ + I_{T-T_0} equal to 10 and 15 kJ/mol are shown.
706 The blue line represents the Sulu UHP-HP metamorphic *P-T* evolution stages from the
707 prograde metamorphic peak at $P \sim 3.5$ GPa and $T \sim 780$ °C (large blue square) to the late
708 stage of exhumation $P \sim 0.3$ GPa and $T \sim 400$ °C (small blue square). The intersection of
709 the calculated equilibrium *P-T locus* of phengite-phlogopite-quartz reaction with the
710 metamorphic path (from Frezzotti et al., 2007) is marked by the blue box.

Phengite megacryst *quasi*-exsolving phlogopite, from Sulu Ultra-high Pressure Metamorphic Terrane, Qinglongshan, Donghai County (eastern China): new data for *P-T-X* conditions during exhumation

Nadia Curetti[a], Costanza Bonadiman [b], Roberto Compagnoni[a,] Luca Nodari[c], Ingrid Corazzari[d,e] , Alessandro Pavese[a]

[a] Department of Earth Sciences, University of Turin, 10125 Turin, Italy

[b] Department of Physics and Earth Sciences, University of Ferrara, 44122 Ferrara, Italy

[c] Institute of Condensed Matter Chemistry and Technology for the Energy– CNR – Padua, Italy

[d] Department of Chemistry, University of Turin, 10125 Turin, Italy

[e] "G. Scansetti" Interdepartmental Center for Studies on Asbestos and Other Toxic Particulates, Turin, Italy.

key-words: phengite and phlogopite micas, exolution reactions, Sulu UHP metamorphic terrane, alkali-alumino-silicate high pressure fluids.

corresponding author: Costanza Bonadiman (bdc @unife.it)

In memory of Prof. Xu Shutong

Abstract

A large crystal of trigonal phengite (*Phe-3T*; $K_{0.96}Na_{0.02}Ba_{0.01})(Al_{1.35}Mg_{0.40}Fe^{2+}_{0.11}Fe^{3+}_{0.13}Ti_{0.02})_{\Sigma=2.02}[Si_{3.44}Al_{0.56}]O_{10}(OH)_2$), sampled from a phengite+quartz metamorphic vein in the eclogites-bearing rocks of Sulu UHP metamorphic terrane, exhibits unusual thin lamellae of ferrian-aluminian trigonal/monoclinic phlogopite polytypes (*Phl-3T*: $(K_{0.78}Na_{0.01})(Mg_{1.48}Fe^{2+}_{0.39}Fe^{3+}_{0.45}Al_{0.30}Ti_{0.06})_{\Sigma=2.68}[Si_{2.98}Al_{1.02}]O_{10}((OH)_{1.77}F_{0.23})$; *Phl-1M*: $(K_{0.85}Ca_{0.01})(Mg_{1.43}Fe^{2+}_{0.45}Fe^{3+}_{0.54}Al_{0.21}Ti_{0.06})_{\Sigma=2.69}[Si_{2.88}Al_{1.12}]O_{10}((OH)_{1.99}F_{0.01})$). This assemblage is rarely observed in UHP eclogite-bearing rocks, and has never been reported before in the Sulu UHP metamorphic terrane. A detailed crystal-chemical characterisation of *Phe-3T*, *Phl-3T* and *Phl-1M* allowed the development of a thermodynamic model that estimates the *P-T* conditions of formation of such an assemblage and helps to understand the relationship between mica polytypes and a quartz dominated (silica oversaturated) system, which characterized the Sulu vein. *Phe-3T* varies in composition upon approaching *Phl-3T*/*1M*, showing a decrease of Si and Al and an increase of Fe and Mg contents. Observed phlogopites cannot be ascribed to bare exsolving processes, and require the involvement of a non-isochemical reaction, dominated by exsolution (*quasi*-exsolution process) in combination with a contribution from an "external chemical supplier" (most probably provided by circulating fluids). Mass balance calculations between the mineralogical assemblage of Sulu vein and the solute components of alkali-alumino-silicate high pressure fluids demonstrate that a silicic-type major element composition accounts for a phengite-quartz based rock. The occurrence of phlogopite micas can be explained as an effect of disproportion in combination with supply components, *i.e*. Mg, Al and K, from alkali-alumino-silicate high pressure fluids.

On the basis of energy modelling of the reaction process from phengite to phlogopite in presence of quartz and a matter exchanger, we determined that such a transformation is weakly dependent on *T* over the 500-930° C thermal range. The intersection of the calculated *P-T* assemblage equilibrium curve with the country rock *P-T* metamorphic path occurs at *P*~2.4±0.2 GPa and *T* ~ 700° C, thus reflecting an early stage of exhumation, close to the metamorphic peak of the Sulu UHP terrane.

1. Introduction

During prograde metamorphism, veins promoted by the availability of the fluid released by the dehydration reactions accompanying temperature (and pressure) increase are ubiquitous (Cong et al. 1994; Zheng et al., 2005). In case of decarbonation reactions, CO_2 also occurs in the fluid phase and carbonate minerals may form in place of or together with silicates. The vein mineral assemblage, which reflects the occurring *P-T-X* conditions at the time of its formation, is useful to infer the metamorphic path experienced by a rock during the whole tectonic evolution. Usually, a close relationship exists between the country rock and the mineralogical composition of the metamorphic vein: *e.g.*, in low-grade metapelites, most metamorphic veins consist of quartz and/or low-temperature minerals such as Fe-rich chlorite and epidote (Hermann and Rubatto, 2009).

Conversely to a widespread opinion that eclogites form at dry conditions or at very low water activity, metamorphic veins involving fluids are not unusual in the HP (high pressure) and UHP (ultra-high pressure) eclogite-facies (Poli and Fumagalli, 2003). For example, in eclogites quartz-rutile veins are ubiquitous, and they were used to estimate the metamorphic temperatures by means of the oxygen isotopes partitioning (*e.g.*, Desmons and O'Neill, 1978).

Good examples of such HP veins in subducted continental crust are found in the "Eclogitic Micaschist Complex" of the Sesia Zone, Western Alps, where quartz veins may include rutile crystals, more than 20 cm long (Compagnoni et al., 2014 and references therein). In the same unit, a metamorphic vein was found, 1-2 m thick and more than 80 m long, mainly consisting of phengite and minor quartz: the phengite flakes, which are up to 30 cm wide, show a unique oscillatory zoning and the coexistence of 3*T* and $2M_1$ polytypes, and no evidence of phlogopite polytypes (Ivaldi et al., 2001).

In the HP/UHP eclogites of the Dabie-Sulu orogenic belt, in addition to the ubiquitous quartz-rutile veins, quartz+zoisite+kyanite veins were found in the Zhu-Jia-Chong eclogite body, where the vein minerals may also attain a pegmatoid size (Castelli et al., 1998). It was proposed that such veins were formed in a closed system during the breakdown of lawsonite which resulted in a kyanite +zoisite +hydrous fluid, either before peak metamorphic conditions (Castelli et al., 1998) or during exhumation (Li et al., 2005).

These metamorphic veins are quite different from veins formed by partial melting during exhumation, which are characterised by a mineral assemblage that reflects the minimum melting granite, *i.e*. the ubiquitous presence of feldspars and mineral grain-size of the order of millimetres (Deng et al., 2017 and references therein).

The phengite specimen under investigation was sampled from a phengite+quartz metamorphic vein, excavated at Qinglongshan, very close to the G30 Lianhuo Expressway, crossing the Donghai County (eastern China). The phengite was collected in a small dump derived from a vertical shaft, excavated in the eclogites-bearing rocks of Sulu UHP metamorphic terrane to mine pure quartz (Fig. 1).

The peak conditions of the UHP metamorphism of the Qinglongshan rocks were estimated at T~700-800°C and P>2.8 GPa (Hirajima and Nakamura, 2003; Liu et al., 2015; Xu et al.,

2012; Zhang et al., 1995) and several *P-T* paths have been suggested (*e.g.*, Ferrando et al., 2005; Frezzotti et al., 2007).

The phengite sample consists of a single undeformed platy crystal, about 520 cm^3 in volume, with a dusky yellowish green colour (Rock Colour Chart, 1991), and it shows the unusual thin lamellae of Fe-phlogopite.

The coexistence of phengite and phlogopite is rarely observed in UHP eclogite-bearing rocks (*e.g.*, Eastern Alps; Eclogite Zone, Tauern, Austria; Frank et al.,1986) and, to the authors' knowledge, has never been reported from Sulu UHP terrane.

The condition and nature of the reactions that lead to the equilibrium of phengite with phlogopite (Zanazzi and Pavese, 2002) upon decreasing pressure are still poorly defined. Melting experiments, conducted on the synthetic K_2O-MgO-Al_2O_3-SiO_2-H_2O (KMASH) system (Massonne and Szpurka, 1997; Thomsen and Schmidt, 2008) and on natural carbonate-bearing eclogites (Droop et al., 1990; Zhang et al., 1995), suggest that a silicate melt at $P > 2$ kbar and $600° < T < 700°C$ produces volatile-rich phases, among which phengite plays a relevant role as potassic mineral (Hermann and Green, 2001; Massonne and Szpurka, 1997; Schmidt and Poli, 1998;; Schmidt et al., 2004).

In view of this, the finding in a quartz+mica assemblage of a large crystal of phengite together with seemingly exsolved phlogopite motivated the present investigation. Note that, an exsolving process in a closed system alone cannot account for the coexistence of phengite and phlogopite, and complex metasomatic reactions involving fluids are also to be assumed. The aim of this work is to provide a thermodynamic model that estimates the *P-T* of formation, starting from a detailed crystal-chemical characterisation of the involved micas.

Phengites (*Phe*) are dioctahedral micas (ideal composition: $KAl_{2-x}(Fe, Mg)_x[Si_{3+x}Al_{1-}$

$_x]O_{10}(OH)_2$) that usually occur in nature as $2M_1$ (more abundant) and 3*T* polytypes (S.G. *C*2/*c* and $P3_112$, respectively). Several 3*T* structures were refined and reported in literature (Amisano-Canesi at al., 1994; Ivaldi et al., 200; Pavese et al., 1997, 1999, 2000, 2003a; Smyth et al., 2000;Weiss et al., 1993), although special attention must be paid to the reliability of the occupancy factors (Pavese and Diella, 2013). Because of its occurrence in high-pressure metamorphic rocks, the 3*T* polytype is thought to be more suitable for high *P* conditions than $2M_1$.The 3*T* polytype presents two independent occupied octahedral-sites (Ferraris et al., 1995; Ferraris and Ivaldi, 2002) while the $2M_1$ only shows one. The 3*T* to $2M_1$ transition is supposed to take place upon decreasing the *P*/*T* ratio (Ivaldi et al., 2001; Sassi et al., 1994). The occurrence of one polytype instead of the other is useful in constraining the pressure-temperature conditions of formation.

In the metamorphic dioctahedral micas, the ^{IV}Si content increases with increasing crystallisation pressure. Single crystals of quartz platelets, 100-700 Å thick, were observed, along with talc, in a phengite coming from the UHP Brossasco-Isasca Unit of southern Dora-Maira Massif, Western Italian Alps (Ferraris et al., 2000). Their occurrence was related to an intra-crystalline re-organisation during decompression of the original phengites.

Phlogopites (*Phl*) are trioctahedral micas (ideal composition $KMg_3[Al\ Si_3]O_{10}(OH)_2$) that usually crystallise as 1*M* (S.G. *C*2/*m*) and rarely as 3*T* (S.G. $P3_112$) polytypes. Only two phlogopites 3*T* were refined and reported in literature: the first one comes from Traversella - Western Alps (Gatta et al., 2011) and the second from Kasenyi – Uganda (Schingaro et al., 2013).

A miscibility gap between dioctahedral and trioctahedral micas is known. Lester (1946) and Gresen et al. (1971) described exsolutions in micas coming from Mitchell Creek

(Georgia, USA). The quoted authors observed unusual and pyramidal intergrowths of biotite in muscovite. Two instances of transmission electron microscopy investigations on trioctahedral exsolutions in magmatic muscovite $2M_1$ were reported: very small exsolutions (~10nm scale) in muscovite from Lawler Peak granite -Arizona (Ferrow et al., 1990) and ferro-aluminian phlogopitic lamellae (~1mm scale) in muscovite from pegmatite outcropping near Gorduno -Switzerland (Ferraris et al., 2001). Experimental studies in the system K_2O-M^{2+}-Al_2O_3-SiO_2-H_2O±(HF) with M^{2+}=Mg^{2+} or Fe^{2+} at *P*~ 2 kbar and variable *T* (200-700°C) showed a relevant dependence of the solid solution stability on temperature (Monier and Robert, 1986a, 1986b).

Understanding the principles underlying the coexistence of the observed phengite and phlogopite in a quartz dominated (silica oversaturated) mineral assemblage of the Sulu vein, will shed light on the "peculiar" *P-T-X* conditions and evolution of the process involved in their formation.

2. Materials and Methods

2.1. Sample Description

The original specimen is a large, flat, regular flake (about 20 cm ×15 cm × 2 cm) of a seemingly hosting phengite mica, characterised by a homogeneous deep green colour. Optical observations and single crystal X-ray rotation photos were performed on several samples extracted from different regions of the phengite mica. They confirmed an overall homogeneous trigonal symmetry of the phengite mica (Fig. 2).

In some areas of the sample, especially near the margins of the flake, associations of quartz and brown micas were observed (Fig. 3). Their nucleation and growth are clearly

163 successive to the hosting phengite crystallisation, because of the preserved iso-orientation
164 of the (001) plane in both hosted- and hosting-micas. This suggests the occurrence of
165 exsolving processes, with the contribution from an "external chemical supplier" (most
166 probably ascribable to fluid circulation). Therefore, the term "*quasi*-exsolution" is used
167 hereafter to address a non-isochemical exsolution process. Such *quasi*-exsolved micas have
168 sub-millimetre extension and micrometre thickness; their shape can be euhedral and
169 pyramidal (Lester, 1946. Fig. 2), or irregular (Fig. 3). Several *quasi*-exsolved mica samples
170 were extracted and tested by single crystal X-ray rotation photos. Most of the specimens
171 are trigonal, and only a few present monoclinic symmetry.
172
173 *2.2 Analytical methods*
174 A fragment of the original mica-matrix sample was grounded to carry out preliminary X-
175 ray powder diffraction characterisations. The measurements were performed by a Huber-
176 Guinier 670 camera, CuKα radiation, scan range $2°<2\theta<70°$ and the diffraction patterns
177 were processed by the GSAS Software Package.
178 The combination of X-ray powder diffraction, optical observations and chemical
179 composition from micro-analyses, revealed the simultaneous occurrence of a major
180 phengite (hereafter *Phe-3T*) and two minor phlogopite polytypes (*Phl-3T* and *Phl-1M*, for
181 trigonal and monoclinic *quasi*-exsolved phlogopites, respectively). Single crystal
182 specimens were separated for X-ray diffraction, which was performed at room temperature
183 using MoKα radiation by both a Siemens P4 diffractometer, equipped with a point detector
184 (University of Turin), and a Gemini R Ultra X-ray diffractometer, equipped with a Ruby
185 CCD detector (CrisDi Interdepartmental Center for Crystallography, University of Turin).
186 The former was used to measure lattice parameters of the samples under investigation; the
187 latter to record diffraction intensities. Because of the limited crystal thickness, the *quasi*-

188 exsolved crystals provided a comparatively small number of *hkl*-reflections. Structure
189 refinements have been performed using both SHELXL-97 package (Sheldrick, 1997) and
190 Jana2006 software (Petricek et al., 2014). *Phl-3T* data allowed a structure refinement using
191 isotropic atomic displacement parameters, only. Single crystal X-ray diffraction
192 experimental setup, overall refinement conditions and lattice parameters of each phase are
193 reported in Table S1.
194 Four fragments from different areas of the original hosting-phengite flake were embedded
195 in epoxy resin and analysed to determine their for chemical composition. Major element
196 compositions were obtained by an ARL-SEMQ electron microprobe analyser (EMPA)
197 equipped with wavelength- and energy-dispersive spectrometers (University of Modena
198 and Reggio Emilia). The following operating conditions were set: 15 kV and 20 nA beam
199 current. Quartz (Si), corundum (Al), periclase (Mg), magnetite (Fe), rhodonite (Mn),
200 grossular (Ca), rutile (Ti), chromium oxide (Cr), vanadinite (V), albite (Na), apatite (P)
201 have been used as standards for the elements in parentheses.
202 Mössbauer spectroscopic analyses were performed on the *Phe-3T* sample in order to
203 quantify Fe^{2+} and Fe^{3+}. The spectrum was collected at room temperature on about 80 mg of
204 powdered sample (Fig. 4), by a conventional constant acceleration spectrometer, using a
205 rhodium matrix ^{57}Co source, nominal strength 1850 mBq (University of Padua). To reduce
206 the crystal iso-orientation, a ‘‘magic angle’’ setting was used (54° between the incident
207 beam and the sample plain). The hyperfine parameters isomer shift (δ), quadrupole
208 splitting (Δ), full linewidth at half maximum (Γ), were expressed in mms−1 while the
209 relative area (A) in %. The parameters were obtained by means of standard least-squares
210 minimiaation techniques. The spectra were fitted to Lorentzian line shapes with the
211 minimum number of doublets. δ is quoted to α-Fe, using a 4-lines calibration.

The water content was assessed by means of thermogravimetric analyses (TGA). TG analyses were carried out under dynamic nitrogen atmosphere (35 mL min^{-1}) by a Pyris 1 ultra-micro-balance - Perkin Elmer. The sample was heated in the temperature range 30-1000 °C (heating rate 20 °C min^{-1}) and an overall weight loss of 4.5% was observed. A first process, observed between 30 and 180 °C, was responsible for a weight loss of 0.5% and was attributed to the desorption of physisorbed water. From 180°C the sample continuously lost weight up to 980 °C due to a not well defined process which was responsible for a weight loss of 4% and was reasonably attributed to the evolution of structural water.

3. Results

Phe-3T and *quasi*-exsolved *Phl*-phases major element compositions are reported in Table 1, whereas the doublets best fit parameters of Mössbauer patterns are listed in Table S2. On the basis of EMPA and Mössbauer analyses, the chemical formula unit of *Phe-3T* (calculated according to 22 negative charges) is:

$(K_{0.96}Na_{0.02}Ba_{0.01})(Al_{1.35}Mg_{0.40}Fe^{2+}_{0.11}Fe^{3+}_{0.13}Ti_{0.02})_{\Sigma=2.02}[Si_{3.44}Al_{0.56}]O_{10}(OH)_2$.

Quantitative chemical analyses performed on the *Phl-3T* specimens provided the following chemical formula unit:

$(K_{0.78}Na_{0.01})(Mg_{1.48}\ Fe^{2+}_{0.39}Fe^{3+}_{0.45}Al_{0.30}Ti_{0.06})_{\Sigma=2.68}[Si_{2.98}Al_{1.02}]O_{10}((OH)_{1.77}F_{0.23})$.

Comparing the two compositions, *Phl-3T* is consistently richer in Fe and Mg than *Phe-3T*, but the $^{VI}Mg/^{VI}Fe$ ratio in the two phases is similar [$(^{VI}Mg/^{VI}Fe)_{Phe\text{-}3T}$ = 1.70, $(^{VI}Mg/^{VI}Fe)_{Phl\text{-}3T}$ = 1.63].

The analyses on the *quasi*-exsolved monoclinic polytype, *Phl-1M*, provided a chemical

composition very close to the trigonal polytype's:

$(K_{0.85}Ca_{0.01})(Mg_{1.43} Fe^{2+}_{0.45}Fe^{3+}_{0.54}Al_{0.21}Ti_{0.06})_{\Sigma=2.69} [Si_{2.88}Al_{1.12}]O_{10}((OH)_{1.99}F_{0.01})$.

Changes of composition from *Phe-3T* to its phlogopite *quasi*-exsolved products were measured along radial directions departing from the separation edge (Fig. 5). A shell with variable width (~300-500 µm) and zoned composition was found: approaching the *quasi*-exsolved phases, Si and Al decrease, while Fe and Mg increase (Table 1; Fig.5). Midway along the transition region from phengite to phlogopite, the following approximated composition occurs:

$(K_{0.89}Na_{0.02}) (Al_{1.24}Fe_{0.52}Mg_{0.54}Ti_{0.02})_{\Sigma=2.32} [Si_{3.16}Al_{0.84}] O_{10}(OH)_2$.

The compositions of *Phl-1M* and *Phl-3T* correspond in micas' nomenclature (Rieder et al., 1998) to "ferrian aluminian phlogopite"; abbreviated to "phlogopite" in the rest of the study.

3.1 Phe-3T and Phl-polytypes

3.1.1 Phe-3T

The average distances <T1-O> and <T2-O> are equal (1.631(1) Å; Tables S3 and S4) and in agreement with literature values. The ditrigonal rotation (Table S5) of the tetrahedral sheet (~4.48°) is in keeping with a HP regime (Curetti et al., 2008).

The average distances <M2-O> and <M3-O> are meaningfully different (1.958(1) Å and 1.972(1) Å, respectively) and indicate a partial octahedral ordering of large cations in M3, although the refined number of electrons (14.3(2) *e* and 14.7(2) *e* in M2 and M3, respectively; Table S3) cannot confirm this inference from bond-lengths.

Mössbauer spectroscopy suggests partial octahedral ordering of iron: (i) Fe^{3+} absorption is

modelled by only one doublet, which suggest that the trivalent iron is completely ordered in one octahedron (0.13 Fe^{3+} a.p.f.u.); (ii) Fe^{2+} absorption is fitted by two doublets, each corresponding to one site (0.05 and 0.06 Fe^{2+} a.p.f.u.). Several Mössbauer analyses on dioctahedral micas $2M_1$ were reported in literature (Aldrige et al., 1987; Finch et al., 1982; Goodman, 1976; Shabani et al., 1998). The patterns usually show two different doublets for Fe^{2+}, even if they are expected to have only one occupied symmetry independent octahedral site. To explain the unexpected second doublet (very weak and corresponding to 0.03-0.04 Fe^{2+} a.p.f.u., at most) the quoted authors assumed a partial occupancy of the M1–*trans* site. The 3*T* polytype has two independent octahedral sites (M2 and M3) and the two Fe^{2+} doublets can be assigned without resorting to the M1 empty site (Merli et al., 2009; Pavese et al., 2000; Pavese et al., 2001;). In fact, partial and very low M1 occupancy is suggested by both chemical analyses (octahedral cations sum = 2.02 a.p.f.u.) and structural refinement (0.86 *e* in the Fourier difference, 0.3(1) *e* refined), though the electron content corresponding to each Mössbauer doublet is too high in comparison with the M1 refined occupancy (0.05 a.p.f.u. corresponding to about 1.3 *e*). Mössbauer spectroscopy is not able to univocally associate iron doublets to specific sites, however its combination with structure refinements allows one to infer a partially ordered distribution of Fe, Al and Mg. The M1 octahedral site is almost completely empty. The H atom position was determined by the Fourier Difference and refined; the O-H distance is 0.80(4) Å and the angle between O-H bond and (0 0 1) plane is ~6.55°.

3.1.2 Phl-3T

Several crystals of phlogopite *3T* were sampled from the hosting phengite *Phe-3T*, but only a few were suitable for measurements and structure refinements. Such specimens are about

200-400 µm in length and width, and very thin (<50 µm). A modest number of reflections were measured for *Phl-3T* and the structural refined parameters show large uncertainties, as shown in the figure of merit reported in Table 1, i.e. $R[|F_o| > 4\sigma(|F_o|)]=8.50\%$. Therefore structure constraints were introduced in the refinement strategy. The atomic displacement parameters have been constrained as follows: $U_{iso}(M1) = U_{iso}(M2) = U_{iso}(M3)$, $U_{iso}(T1) = U_{iso}(T2)$, $U_{iso}(O1) = U_{iso}(O2) = U_{iso}(O3) = U_{iso}(O4) = U_{iso}(O5) = U_{iso}(O6)$ (Table 4). Conversely, the fractional coordinate distances were refined without any constraint, and the cation-anion distances were determined accordingly.

The structural results can be compared with those of the trigonal phlogopite samples from Traversella (*Phl*-TR) and from Uganda (*Phl*-UG). In *Phl*-TR <M1-O> is 2.079 Å, and 2.072(6) Å in *Phl*-UG. In both samples, <M1-O>s are not significantly different from <M2-O> and <M3-O>. Conversely, the trigonal phlogopite sample investigated here, exhibits <M1-O> of 2.245(3) Å, some 10% longer than <M2-O> = 1.991 (8) Å and <M3-O> = 2.052(8) Å (Table S4).

The occupancy factors of Fe-Al-Mg-Si in the tetrahedral and octahedral sites were not refined and the cations were arranged according to a completely disordered distribution. Only the number of electrons in the interlayer site was refined, as 16.9(2) *e*.

Comparing the distortion parameters (Table S5) with those reported for *Phl*-TR/UG, *Phl-3T* is more strained. Such an aspect is more marked in *Phl*-UG. The major distortions are not related to bond lengths, but mainly to angular values, thus suggesting that the structure strain is probably due to the *Phl-3T*'s growth process, which took place as a progressive substitution of the pre-existing framework of *Phe-3T*.

307 *3.1.3 Phl-1M*

308 Only a few specimens of monoclinic *quasi*-exsolved phase were found in the hosting
309 phengite. Using the largest one we performed single crystal X-ray diffraction experiments
310 with a satisfactory number of reflections. The structure refinement in the S.G. *C*2/*m*
311 converged to R ~ 4.78% (Table S3).

312 The cell parameters (a = 5.3195(13) Å, b = 9.2117(12) Å, c = 10.210(3) Å, β = 100.04(2)°,
313 V = 492.7(2) Å^3; Table S4) are in excellent agreement with the ones of *Phl-3T* (a =
314 5.318(1) Å, c = 30.21(2) Å; $c_{(1M)} \times \text{sen}\,\beta_{(1M)}$ = 30.16 Å).

315 Average bond distances $\langle T\text{-}O\rangle_{1M}$ = 1.652(1) Å, $\langle M\text{-}O\rangle_{1M}$ = 2.074(1) Å and $\langle I\text{-}O\rangle_{1M}$ =
316 3.159(1) Å are very similar to the corresponding values in *Phl-3T* sample (Tables S3 and
317 S4). The two M-O distances are meaningfully different from one another (<M1-O> =
318 2.088(1); <M2-O> = 2.061(1) Å), but the refined electron content (14.17(14) and
319 14.18(12) *e* for M1 and M2, respectively) does not indicate any cation order.

320 *Phl-1M* yields bond-lengths, bond-angles and distortion parameters (α=8.00°, Δz=0.01Å;
321 Δ_{TM} = 0.44Å, BLD_{M1} = 0.76%, BLD_{M2} = 0.80%, J_{M1} = 0.00° and J_{M2} = 0.88°; Table S5) in
322 agreement with those reported in literature on phlogopite 1*M* (Brigatti and Guggenheim,
323 2002).

324

325 **4. Discussion**

326

327 *4.1 Mass balance calculation*

328 The rock containing the studied micas and quartz is a thick metamorphic vein, similar to
329 those commonly observed in the Sulu UHP terrane. A not-weighted mass balance
330 calculation (Wright and Doherty, 1970) was used to provide the best match between the

sampled mineralogical assemblage and fluid alkali-alumino-silicate components that mirror the bulk rock averaged compositions of the Sulu-vein (*ASV*), reduced to an anhydrous major oxides system (Table 2):

x_1 *Phe-3T* + x_2 quartz + x_3 *Phl-3T* + x_4 *Phl-1M* + x_5 K-feldspar = 1 *ASV* (1)

where x_i represents the *i*-phase proportion. The solution is (least square residuum, r^2=0.8):

0.574 *Phe-3T* + 0.488 quartz + (-0.049) *Phl-3T* + (-0.002) *Phl-1M* + (-0.001) K-feldspar =1 *ASV* (2)

Eq.(2) demonstrates that *ASV* accounts for a phengite-quartz based rock and the occurrence of phlogopite micas can be explained as an effect of disproportion in combination with a supply of elements, *i.e.* Mg, Al and K, most probably solute components of alkali-alumino-silicate aqueous solutions at high pressure rock-fluid interactions.

Such results agree with the observed petrographic characteristics of the vein fragment from which the studied micas were extracted: (1) phengite and quartz are comparably proportioned in the rock; (2) the negative phase proportion coefficients suggest that phlogopites are *per force* scarce and only occur as *quasi*-exsolved phases, in combination with an elemental supply from alkali-alumino-silicate high pressure fluids; (3) K-feldspar is modally absent in the fragment, as the negligible resulting negative proportion (*i.e.* -0.001) suggests.

4.2 *P-T-X Equilibrium phases in an open system*

The coexistence of *Phe-3T, Phl-3T* and *Phl-1M* micas cannot be reduced to bare exsolving reactions in a closed system and a contribution from an "external chemical supplier", *i.e.* a "*reservoir*", has to be taken into account (eq.(2)). Therefore, the reactions were modelled

in terms of an open system. Following Merli et al. (2017), the "reservoir" is now seen as a matter exchanger, whose composition, addressed by *Res*(A/B), encompasses all the potential solids and fluids taking part in the petrogenetic reactions, but micas and quartz. A/B are used to indicate a specific chemical condition of the reservoir. In this case, we modelled the reaction process from phengite to phlogopite with the following transformation:

phengite + *Res*(A) = phlogopite +λ quartz + *Res*(B) (3)

where λ is related to the amount of quartz exsolved from the reacting phengite, *i.e.* λ≈0.46. The equilibrium conditions of the assemblage require that

$$\Delta G = G(\text{phengite}) + G[Res(\text{A})] - G(\text{phlogopite}) - G[Res(\text{B})] - \lambda\, G(\text{quartz}) =$$

$$G(\text{phengite}) - G(\text{phlogopite}) - \lambda\, G(\text{quartz}) + \{G[Res(\text{A})] - G[Res(\text{B})]\} =$$

$$G(\text{phengite}) - G(\text{phlogopite}) - \lambda\ G(\text{quartz}) + \delta G[Res] = 0\ , \qquad (4)$$

where G is the molar Gibbs energy of a given phase, *i.e.* its chemical potential, and $\delta G[Res]$ is the molar Gibbs energy difference between *Res*(A) and *Res*(B). Phengite and phlogopite refer to *Phe-3T* and *Phl-3T*, respectively.

The Gibbs energy of a phase at given *P*-*T* conditions can be determined by two distinct integrations, one along an isobar at P_0 and the other along an isotherm at *T*, *i.e.*

$$G(P,T) = G(P_0,T_0) - \int_{T_0}^{T} S\,(P_0,T')dT' + \int_{P_0}^{P} V(P',T)dP' \qquad (5)$$

where P_0 and T_0 are in general reference pressure and temperature (for explicit calculations refer to Pavese and Diella, 2007), here corresponding to room pressure and temperature. Equation (5) can be written as

$$\Delta G(P,T) = \Delta G(P_0,T_0) + \Delta I_{T-T_0} + \Delta I_{T-T_0,\text{config}} + \Delta I_{P-P_0}. \qquad (6)$$

where $\Delta G(P_0,T_0)$ is the formation energy with respect to the standard state of the constituent oxides. ΔI_{P-P_0} is due to the solid phases of eq. (4), *i.e.* micas and quartz, and it

379 can be determined by means of the equations of state of the involved minerals. We used a
380 third order Birch-Murnaghan *P-V-T* relationship and thermo-elastic parameters from
381 Amisano-Canesi et al. (1994); Angel et al. (1997); Chon et al. (2003, 2006); Comodi et
382 al. (1999); Curetti et al. (2006); Gatta et al. (2009, 2011), Gemmi et al. (2008). Hazen
383 and Finger (1978); Russell and Guggenheim (1999); Takeda and Morosin (1975) and
384 Ventruti et al. (2009).
385 $\Delta G(P_0, T_0)$ + I_{T-T_0} were estimated by the reaction:
386 $\frac{1}{2}$ muscovite + $\frac{1}{4}$ celadonite + $\frac{1}{4}$ Fe − celadonite + 1.75 periclase + 0.75 wüstite =
387 $\frac{2}{3}$phlogopite + $\frac{1}{3}$ annite + $\frac{1}{2}$corundum + $\frac{1}{2}$quartz
388 taking the Gibbs energy of formation and heat capacity at constant pressure from Holland
389 and Powell (1998). The $\Delta G(P_0, T_0)$ + I_{T-T_0} is modest and weakly dependent on *T* in the
390 investigated 770-1200 K thermal range. In was therefore approximated by a constant as
391 large as 13 kJ/mol. However, taking into account the high degree of approximation, we
392 assumed a confidence range from 10 to 15 kJ/mol, and explored its limits. Lastly,
393 $\Delta I_{T-T_0,\text{config}}$ is due to the configuration contribution to entropy, S_{config}, which is calculated
394 as follows:
395 $$S_{\text{config}} = -\text{R}\sum_{j=1}^{sites}\sum_{\alpha=1}^{chemical\ species} p_{j,\alpha}\ln\left(p_{j,\alpha}\right)$$
396 where R is the universal gas constant and $p_{j,\alpha}$ is the occupancy factor of the α–species at
397 the j^{th}-sites. In figure 6 we display the *P-T loci* (GPa and °C) of equilibrium for reaction
398 (4), with $\Delta G(P_0, T_0)$ + I_{T-T_0} equal to 10 and 15 kJ/mol, respectively.
399 The intersection between the equilibrium *P-T locus* and the supposed *P-T* metamorphic
400 path of OH-rich quartzite from Sulu UHP terrane from Frezzotti et al. (2007) occurs at $P \approx$
401 2.4±0.2 GPa and $T \approx$ 700 °C. Such a result is consistent with the observation of Hermann

and Green (2001), if the phengite existence curve of the quoted authors is extrapolated to 700 °C.

On the basis of petrological data, stable isotope geothermometry and theoretical phase relationships of quartzites from Sulu terrane, the UHP fluids composition estimated by Frezzotti et al. (2007) is an intermediate alkali-alumino-silicate aqueous solutions (H_2O ~50 wt %), that constrains the metamorphic peak at $P \sim 3.5$ PGa and $T \sim 780$ °C .

The obvious compositional similarity between the quartzites investigated by Frezzotti et al. (2007) and the Sulu vein of this study allowed us to state that the calculated P-T conditions for phlogopite growth in a SiO_2 oversaturated system indicate at a region that reflects early stages of exhumation, close to the metamorphic peak (Fig. 6).

5. Conclusions

The main purpose of this work was to study the rare coexistence of dioctahedral mica and trioctahedral *quasi*-exsolutions observed in a thick quartz+phengite metamorphic vein found in the northern part of Sulu UHP metamorphic terrane, of Donghai County (eastern China).

The process leading to such an assemblage is described as a "*quasi*-exsolution" process and it is constituted by non-isochemical exsolution . The composition change is due to an external supplier.

The reaction process from phengite to phlogopite favours /requires the exsolution of quartz. Because of the trigonal structure provided from phengite, the *quasi*-exsolved phlogopite crystallised as *3T*-polytype, which is unusual for trioctahedral micas.

Mass balance calculations suggest that the phengite-quartz based rock and the occurrence of phlogopite micas can be explained as an effect of disproportion in combination with a

supply of elements, *i.e*. Mg, Al and K, from alkali-alumino-silicate high pressure fluids, that mirror the bulk Sulu vein composition.

The calculated equilibrium *P-T locus* of phengite-phlogopite-quartz reaction intersects the *P-T* metamorphic path at $P \approx 2.4 \pm 0.2$ GPa and $T \approx 700$ °C, indicating an early stage of exhumation, close to the metamorphic peak of the Sulu UHP terrane.

Acknowledgements

The studied phengite was collected in 2000, during a field expedition in the Sulu orogene, organised by Prof. Xu Shutong in the framework of a Chinese-Italian cooperation project (R.C The authors thank the Editor Marco Scmbelluri, Patrizia Fumagalli and anonymous reviewer for their positive comments. The authors would like to thank the "Compagnia di San Paolo" of Turin, Italy, for supporting the TGA measurements. L.N would like to thank the Department of Chemical Science, University of Padua, for allowing the free use of Mössbauer spectrometer.

The paper benefited of the English language editing provided by Barbara Galassi (Brighton, U.K)

Part of this research was supported by MIUR-2015 20158A9CBM Grant (C.B).

References

Aldridge, L.P., Finch, J, Gainsford, A.R., Tennant, W.C., Childs, C.W., 1987. Electric-field gradient in muscovites. American Mineralogist 72, 528-536.

Amisano-Canesi, A., Chiari, G., Ferraris, G., Ivaldi, G., Soboleva, S.V., 1994. Muscovite- and phengite-3T: crystal structure and conditions of formation. European Journal of Mineralogy 6, 489-496.

452 Angel, R.J., Allan, D.R., Miletich, R., Finger, L.W., 1997. The use of quartz as an internal
453 pressure standard in high pressure crystallography. Journal of Applied
454 Crystallography 30, 461-466.
455 Brigatti, F., Guggenheim, S., 2002. Mica crystal chemistry and the influence of pressure,
456 temperature, and solid solution on atomistic models. Reviews in Mineralogy and
457 Geochemistry 46, 1-97.
458 Castelli, D., Rolfo, F., Compagnoni, R., Xu, S.T., 1998. Metamorphic veins with kyanite,
459 zoisite and quartz in the Zhu-Jia-Chong eclogite, Dabie Shan, China. Island Arc
460 7(1-2), 159-173.
461 Chon C-M, Kim SA, Moon H-S, 2003. Crystal structure of biotite at high temperatures and
462 of heat-treated biotite using neutron powder diffraction. Clays and Clay Minerals
463 51, 519–528.
464 Chon, C.-M., Lee, C.-K., Song, Y., Kim, S.-A., 2006. Structural changes and oxidation of
465 ferroan phlogopite with increasing temperature: in situ neutron powder diffraction
466 and Fourier transform infrared spectroscopy, Physics and Chemistry of Minerals
467 33(5), 289-299.
468 Comodi, P., Zanazzi, P.F., Weiss, Z., Rieder, M., Drábek, M., 1999. “Cs-ferri-tetra-
469 annite”: high-pressure and high-temperature behavior of a potential nuclear waste
470 disposal phase. American Mineralogist 84, 325-332.
471 Compagnoni, R., Engi, M., Regis, D., 2014. Val d’Aosta section of the Sesia Zone: multi-
472 stage H*P* metamorphism and assembly of a rifted continental margin**.** 10th Int.
473 Eclogite Conf., Syn-Conference Excursion, 5 September 2013, GFT – Geological
474 Field Trips, 6 (1.2), 1-44. ISSN: 2038-4947. (DOI 10.3301/GFT.2014.02)
475 http://www.isprambiente.gov.it/it/pubblicazioni/periodici-tecnici/geological-field-

trips/valle-daosta-section-of-the-sesia-zone.

Cong, B.-L., Wang, Q.C., Zhai, M., Zhang, R.Y., Zhao, Z.Y., Ye, K., 1994. Ultrahigh-pressure metamorphic rocks in the Dabishan–Sulu Region of China. Island Arc 3, 135–150.

Curetti, N., Levy, D., Pavese, A., Ivaldi, G., 2006. Elastic properties and stability of coexisting 3T and 2M1 phengite polytypes. Physics and Chemistry of Minerals 32(10), 670 – 678.

Curetti, N., Ferraris, G., Ivaldi, G., 2008. Correlation between crystallization pressure and structural parameters of phengites. American Mineralogist 93, 451-455.

Deng, L.-P., Liu, Y.-C., Gu, X.-F., Groppo, C., Rolfo, F., 2017. Partial melting of ultrahigh-pressure metamorphic rocks at convergent continental margins: Evidences, melt compositions and physical effects, Geoscience Frontiers. http://dx.doi.org/10.1016/j.gsf.2017.08.002

Desmons, J., O'Neill, J.R., 1978. Oxygen and hydrogen isotope compositions of eclogites and associated rocks from the eastern Sesia Zone (Western Alps, Italy). Contributions to Mineralogy and Petrology 67, 79-85.

Droop, G.T.R., Lombardo, B., Pognante, U., 1990. Formation and distribution of eclogite facies rocks in the Alps. In: D.A. Carswell, (Ed.) Eclogite Facies Rocks. Glasgow, Blackie, 225-259.

Ferrando, S., Frezzotti, M.L., Dallai, L., Compagnoni, R., 2005. Fluid-rock interaction in UHP phengite-kyanite-epidote eclogite from the Sulu Orogen, Eastern China. International Geology Review 47, 750-774.

Ferraris, G., Ivaldi, G., 2002. Micas: crystal chemistry and metamorphic petrology. Reviews in Mineralogy and Geochemistry 46, 117-153.

Ferraris, G., Ivaldi, G., Nespolo, M., Takeda, H., 1995. On the stability of dioctahedral

501 micas. Terra Abstract (suppl. N.1 Terra Nova) 7, 289.
502 Ferraris, C., Chopin, C., Wessicken, R., 2000. Nano- to micro-scale decompression
503 products in ultrahigh-pressure phengite: HRTEM and AEM study, and some
504 petrological implications. American Mineralogist 85, 1195-1201.
505 Ferraris, C., Grobety, B., Wessicken, R., 2001. Phlogopite exsolution within muscovite: a
506 first evidence for a higher-temperature re-equilibration, studied by HRTEM and
507 AEM techniques. European Journal of Mineralogy 13, 15-26.
508 Ferrow, E.A., London, D., Goodman, K.S., Veblen, D.R., 1990. Sheet silicates of the
509 Lawler Peak granite, Arizona: chemistry, structural variations, and exsolution.
510 Contributions to Mineralogy and Petrology 105, 491-501.
511 Finch, J., Gainsford, A.R., Tennant, W.C., 1982. Polarized optical absorption and ^{57}Fe
512 Mössbauer study of pegmatitic muscovite. American Mineralogist 67, 59-68.
513 Frank, W., Hock, V., Miller, C., 1986. Metamorphic and tectonic history of the Central
514 Tauern Window. In: H.W. Flugel, P. Faupl (Eds.), Geodynamics of the Eastern
515 Alps, Deuticke, Vienna, 34-54.
516 Frezzotti, M.L., Ferrando, S., Dallai, L., Compagnoni, R., 2007. Intermediate alkali-
517 alumino-silicate aqueous solutions released by deeply-subducted continental crust:
518 fluid evolution in UHP OH-rich topaz-kyanite-quartzites from Donghai County
519 (Sulu, China). Journal of Petrology 48, 1219-1241.
520 Gatta, G.D., Rotiroti, N., Pavese, A., Lotti, P., Curetti, N., 2009. Structural evolution of a
521 3T phengite mica up to 10 GPa: an in-situ single-crystal X-ray diffraction study.
522 Zeitschrift für Kristallographie 224, 302-310.
523 Gatta, G.D., Merlini, M., Rotiroti, N., Curetti, N., Pavese, A., 2011. On the crystal
524 chemistry and elastic behavior of a phlogopite 3T. Physics and Chemistry of

525 Minerals 38, 655-664.
526 Gemmi, M., Merlini, M., Pavese, A., Curetti, N., 2008. Thermal expansion and
527 dehydroxylation of phengite micas. Physics and Chemistry of Minerals 35(7), 367-
528 379.
529 Goodman, B.A., 1976. The Mössbauer spectrum of a ferrian muscovite and its implications
530 in the assignment of sites in dioctahedral micas. Mineralogical Magazine 40, 513-
531 517.
532 Gresens, R.L., Stensrud, H.L., 1971. Chemical, optical, and X-ray analysis of an unusual
533 muscovite-biotite intergrowth. Lithos 4, 63-69.
534 Hazen, R.M., Finger, L.W., 1978. The crystal structures and compressibilities of layer
535 minerals at high pressure. II Phlogopite and Chlorite. American Mineralogist 63,
536 293-296.
537 Hermann, J., Green, D.H., 2001. Experimental constraints on high pressure melting in
538 subducted crust. Earth and Planetary Science Letters 188, 149-168.
539 Hermann, J., Rubatto, D., 2009. Accessory phase control on the trace element signature of
540 sediment melts in subduction zones. Chemical Geology 265, 512–526.
541 Hirajima, T., Nakamura, D., 2003. The Dabie Shan– Sulu orogeny. In: D.A., Carswell and
542 R., Compagnoni (Eds.), Ultrahigh-pressure metamorphism. E.M.U. Notes in
543 Mineralogy 5, 105–144. Eötvös University Press, Budapest.
544 Holland, T.J.B., Powell, R., 1998. An internally consistent thermodynamic data set for
545 phases of petrological interest. Journal of Metamorphic Geology 16, 309-343.
546 Ivaldi, G., Ferraris, G., Curetti, N., Compagnoni, R., 2001. Coexisting 3T and 2M1
547 polytypes of phengite from Cima Pal (Val Savenca, western Alps): Chemical and
548 polytypic zoning and structural characterisation. European Journal of Mineralogy

549 13, 1025-1034.
550 Lester, J.G., 1946. Inclusions in muscovite from Mitchell Creek Mine, Upson Country,
551 Georgia. American Mineralogist 31, 77-81.
552 Li X.-P., Li Y.-L., Shu G.-M., 2005. Breakdown of lawsonite subsequent to peak UHP
553 metamorphism in the Dabie terrane and its implication for fluid activity. Chinese
554 Science Bulletin 50(13), 1366-1372.
555 Liu, Y.-C., Deng, L., Gu, X., Groppo, C., Rolfo, F., 2015. Application of Ti-in-zircon and
556 Zr-in-rutile thermometers to constrain high-temperature metamorphism in eclogites
557 from the Dabie orogen, central China. Gondwana Research 27, 410-423.
558 Massonne, H.-J., Szpurka, Z., 1997. Thermodynamic properties of white micas on the basis
559 of high-pressure experiments in the systems K_2O-MgO-Al_2O_3-SiO_2-H_2O and K_2O-
560 FeO-Al_2O_3-SiO_2-H_2O. Lithos 41, 229-250.
561 Mattinson C.G., Zhang R-Y., Tsujimori T., Liou J.G., 2004. Epidote-rich talc-kyanite-
562 phengite eclogites, Sulu terrane, eastern China: P-T-fO2 estimates and the
563 significance of the epidote-talc assemblage in eclogite. American Mineralogist
564 89(11-12), 1772-1783.
565 Merli, M., Pavese, A., Curetti, N., 2009. Maximum entropy method: an unconventional
566 approach to explore observables related to the electron density in phengites. Physics
567 and Chemistry of Minerals 36, 19-28.
568 Merli, M., Bonadiman, C., Diella, V., Sciascia, L., Pavese, A., 2017. Fe-periclase reactivity
569 at Earth's lower mantle conditions: Ab-initio geochemical modelling. Geochimica
570 et Cosmochimica Acta 214, 14-29.
571 Monier, G., Robert, J.L., 1986a. Muscovite solid solutions in the system K_2O-MgO-FeO-
572 Al_2O_3-SiO_2-H_2O: an experimental study at 2 kbar P_{H2O} and comparison with natural

573 Li-free white micas. Mineralogical Magazine 50, 257-266.
574 Monier, G., Robert, J.L., 1986b. Evolution of the miscibility gap between muscovite and
575 biotite solid solutions with increasing lithium content: an experimental study in the
576 system K_2O-Li_2O-MgO-FeO-Al_2O_3-SiO_2-H_2O-HF at 600°C, 2 kbar P_{H2O}:
577 comparison with natural lithium micas. Mineralogical Magazine 50, 641-651.
578 Pavese, A., Diella, V., 2007. Uncertainties on elastic parameters and occupancy factors:
579 how do they affect the accuracy of the calculated Gibbs energy of minerals at (P,T)
580 conditions? The case of 3T- versus $2M_1$ phengite. Physics and Chemistry of
581 Minerals 34(9), 637-645.
582 Pavese, A., Diella, V. 2013. How stacking disorder can conceal the actual structure of
583 micas: the case of phengites. DOI:10.1007/s00269-013-0568-6. Physics and
584 Chemistry of Minerals 40, 375-386.
585 Pavese., A., Ferraris, G., Pischedda, V., Ibberson, R., 1997. Cation Site ordering in
586 phengite 3T from Dora Maira massif (western Alps): a variable-temperature
587 neutron powder diffraction study. European Journal of Mineralogy 9, 1183-1190.
588 Pavese, A., Ferraris, G., Pischedda, V., Mezouar, M., 1999. Synchrotron powder
589 diffraction study of phengite 3T from Dora Maira massif: P-V-T equation of state
590 and petrological consequences. Physics and Chemistry of Minerals 26, 460-467.
591 Pavese, A., Ferraris, G., Pischedda, V., Radaelli, P., 2000. Further study of cation ordering
592 in phengite 3T by neutron powder diffraction. Mineralogical Magazine 64, 11-18.

593 Pavese, A., Ferraris, G., Pischedda, V., Fauth, F., 2001. M1-site occupancy in 3T and
594 $2M_1$ phengites by low temperature neutron powder diffraction: Reality or artefact?
595 European Journal of Mineralogy 13, 1071-1078.
596 Pavese, A., Curetti, N., Ferraris, G., Ivaldi, G., Russo, U., Ibberson, R., 2003a.
597 Deprotonation and order-disorder reactions as a function of temperature in a
598 phengite 3T (Cima Pal, western Alps) by neutron diffraction and Mössbauer
599 spectroscopy. European Journal of Mineralogy 15, 357-363.
600 Pavese, A., Levy, D., Curetti, N., Diella, V., Sani, A., 2003b. Equation of state and
601 compressibility of phlogopite by in-situ high pressure X-ray diffraction experiment.
602 European Journal of Mineralogy 15, 455-463.
603 Pavese, A., Curetti, N., Diella, V., Levy, D., Dapiaggi, M., Russo, U., 2007. *P-V* and *T-V*
604 Equations of State of natural biotite: an *in-situ* high pressure and high temperature
605 powder diffraction study, combined with Mössbauer spectroscopy. American
606 Mineralogist 92(7), 1158-1164.
607 Petricek, V., Dusek, M., Palatinus, L., 2014. Crystallographic Computing System
608 JANA2006: General features. Zeitschrift für Kristallographie 229(5), 345-352.
609 Poli, S., Fumagalli P., 2003. Mineral assemblages in ultrahigh pressure metamorphism: A
610 review of experimentally determined phase diagrams. In: D.A. Carswell and R.
611 Compagnoni (Eds.) Ultrahigh-pressure metamorphism. E.M.U. Notes in
612 Mineralogy 5, 307-340. Eötvös University Press, Budapest.
613 Rieder, M., Cavazzini, G., D'Yakonov, Yu.S., Frank-Kamenetskii, V.A., Gottardi, G.,
614 Guggenhein, S., Koval, P.V., Müller, G., Neiva, A.M.R., Radoslovich, E.W.,
615 Robert, J.L., Sassi F.P., Takeda, H., Weiss Z., Wones, D.R., 1998. Nomenclature of
616 the micas. The Canadian Mineralogist 36, 905-912.

617 Geological Society of America, 1991: Rock color chart with genuine Munsell^{R} color chips.
618 Boulder, Colo Ed.
619 Russell, R.L., Guggenheim, S., 1999. Crystal structures of near-end-member phlogopite at
620 high temperatures and heat-treated Fe-rich phlogopite: The influence of the O, OH,
621 F site. The Canadian Mineralogist 37, 711-720.
622 Sassi, F.P., Guidotti, C., Rieder, M., De Pieri, R., 1994. On the occurrence of metamorphic
623 2M1 phengites: some thoughts on polytypism and crystallization condition of 3T
624 phengites. European Journal of Mineralogy 6, 151-160.
625 Schingaro, E., Lacalamita, M., Scordari, F., Mesto, E., 2013. 3T-phlogopite from Kasenyi
626 kamafugite (SW Uganda): EPMA, XPS, FTIR and SCXRD study. American
627 Mineralogist 98, 709-717.
628 Schmidt, M.W., Poli, S., 1998. Experimentally based water budgets for dehydrating slabs
629 and consequences for arc magma generation. Earth and Planetary Science Letters
630 163, 361-379.
631 Schmidt, M. W., Vielzeuf, D., Auzanneau, E., 2004. Melting and dissolution of subducting
632 crust at high pressures: the key role of white mica. Earth and Planetary Science
633 Letters 228, 65-84.
634 Shabani, A.A.T., Rancourt, D.G., Lalonde, A.E., 1998. Determination of cis and trans
635 Fe2+ populations in 2M(1) muscovite by Mossbauer spectroscopy. Hyperfine
636 Interactions, 117, 117-129.
637 Sheldrick, G.M., 1997. SHELXL-97, Program for the Refinement of Crystal Structure;
638 University of Göttingen, Germany.
639 Smyth, J.R., Jacobsen, S.D., Swope, R.J., Angel, R.J., Arlt, T., Domanik, K., Holloway,
640 J.R., 2000. Crystal structures and compressibilities of synthetic $2M_1$ and 3T

641 phengite micas. European Journal of Mineralogy 12(5), 955-963.
642 Takeda, H., Morosin, B., 1975. Comparison of observed and predicted structural
643 parameters of mica at high temperature. Acta Crystallographica B31, 2444-2452.
644 Thomsen, T.B., Schmidt, M.W., 2008. The Biotite to Phengite Reaction and Mica-
645 dominated Melting in Fluid+Carbonate-saturated Pelites at High Pressures. Journal
646 of Petrology 49, 1889-1914.
647 Tutti, F., Dubrovinsky, LS., Nygren, M., 2000. High-temperature study and thermal
648 expansion of phlogopite. Physics and Chemistry of Minerals 27(9), 599-603.
649 Ventruti, G., Levy, D., Pavese, A., Scordari, F., Suard, E., 2009. High-temperature
650 treatment, hydrogen behaviour and cation partitioning of a Fe-Ti bearing volcanic
651 phlogopite by in situ neutron powder diffraction and FTIR spectroscopy. European
652 Journal of Mineralogy 21(2), 385-396.
653 Weiss, Z., Rieder, M., Smrcok, L., Petricek, V., Bailey, S.W., 1993. Refinement of the
654 crystal structures of two “protolithionites”. European Journal of Mineralogy 5,
655 493-502.
656 Wright, T.L., Doherty, P.C., 1970. A linear programming and least-squares computer
657 method for solving petrologic mixing problems. Geological Society of America
658 Bulletin 81, 1995–2008.
659 Xu, H.J., Ye, K., Zhang, J.F., 2012. Temperature of prograde metamorphism,
660 decompressional partial melting and subsequent melt fractional crystallization in
661 the Weihai migmatitic gneisses, Sulu UHP terrane: constraints from Ti-in-zircon
662 thermometer. Journal of Earth Sciences 23, 813–827.
663 Zanazzi, P.F. and Pavese, A., 2002. Behavior of micas at high pressure and high
664 temperature. Reviews in Mineralogy and Geochemistry 46, 98-116.

Zhang, R. Y., Hirajima, T., Banno, S., Cong, B., Liou, J. G., 1995. Petrology of ultrahigh-pressure rocks from the southern Sulu region, eastern China. Journal of Metamorphic Geology 13, 659–675.

Zhang, R.Y., Yang, J.S., Wooden, J.L., Liou, J.G., Li, T.F., 2005. U–Pb SHRIMP geochronology of zircon in garnet peridotite from Sulu UHP terrane, China: implications for mantle metasomatism and subduction-zone UHP metamorphism. Earth and Planetary Science Letters 237, 729–743.

Zhang, Z.M., Xiao, Y.L., Liu, F., Liou, J.; Hoefs, J., 2005. Petrogenesis of UHP metamorphic rocks from Qinglongshan, Southern Sulu, East-Central China. Lithos 81, 189-207

Zheng, Y., Zhou, J.-B., Wu, Y.-B., Xie, Z., 2005. Low-grade metamorphic rocks in the Dabie–Sulu orogenic belt: a passive-margin accretionary wedge deformed during continent subduction. International Geology Review 47, 851–871.

678 **Figure 1.** Simplified geologic sketch map of the Sulu orogen showing major tectonic units.
679 YQWF, Yantai-Qingdao-Wulian fault White circles mark the location of labelled towns
680 (from Mattinson et al., 2004 and Zhang et al., 2005, modified); The phengite+quartz
681 metamorphic vein was excavated at Qinglongshan (evidenced in the map), in the Donghai
682 County.
683
684 **Figure 2.** Optical micrograph (plane polarised light) of Fe-phlogopite *quasi*-exsolution
685 (brown colour) developed in pyramidal form (its thickness increases toward the centre),
686 with several evident growth stages.
687
688 **Figure 3**. Optical micrographs of mica *quasi*-exsolutions and quartz crystals in trigonal
689 phengite observed under plane polarised (a) light and crossed polarised (b) lights,
690 respectively. The *quasi*-exsolution is apparent in (a) (darker portions) while the mica-
691 quartz reaction is amplified in (b) (white portions).
692
693 **Figure 4**. Mössbauer spectrum collected on *Phe-3T* sample. The peaks are fitted with three
694 doublets and they indicate that 57(1)% of the total Fe is trivalent, 43(1)% bivalent
695 (parameters in Table S1).
696
697
698 **Figure 5**. Changes of chemical composition from *Phe-3T* to *Phl-3T*; (a) schematic
699 representation of the analysed sample and location of the analysis points. (b) The
700 histogram reports the variation by weight % of the principal oxides; approaching the *quasi*-
701 exsolved phases, Si and Al decrease, while Fe and Mg increase.

Figure 6. Pressure-temperature loci of equilibrium for the phengite-phlogopite-quartz reaction (eq. 2). The cases of $\Delta G(P_0, T_0)$ + I_{T-T_0} equal to 10 and 15 kJ/mol are shown. The blue line represents the Sulu UHP-HP metamorphic *P-T* evolution stages from the prograde metamorphic peak at $P \sim 3.5$ GPa and $T \sim 780$ °C (large blue square) to the late stage of exhumation $P \sim 0.3$ GPa and $T \sim 400$ °C (small blue square). The intersection of the calculated equilibrium *P-T locus* of phengite-phlogopite-quartz reaction with the metamorphic path (from Frezzotti et al., 2007) is marked by the blue box.

Figure 1

Click here to download high resolution image

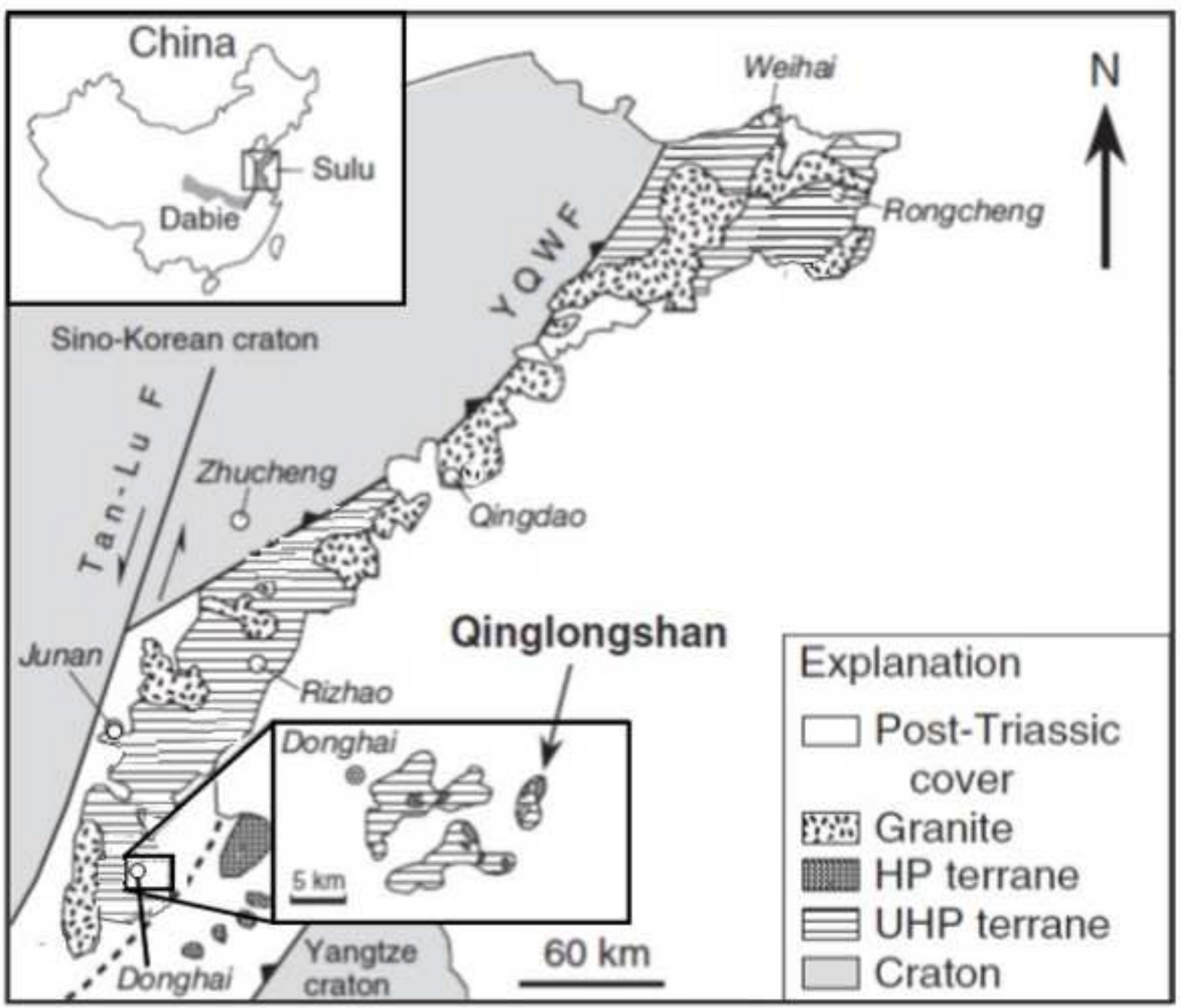

Figure 2

Click here to download high resolution image

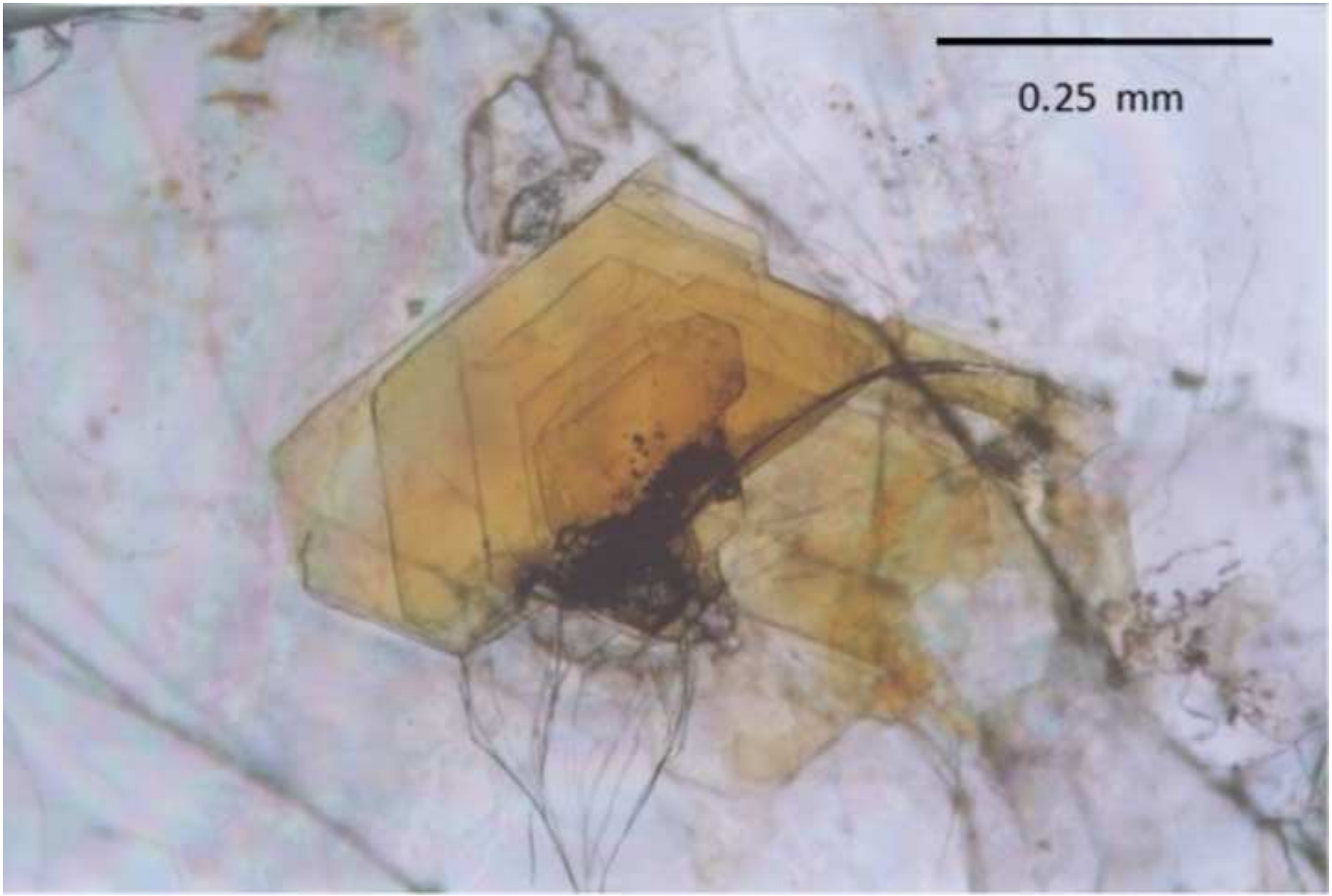

Figure 3

Click here to download high resolution image

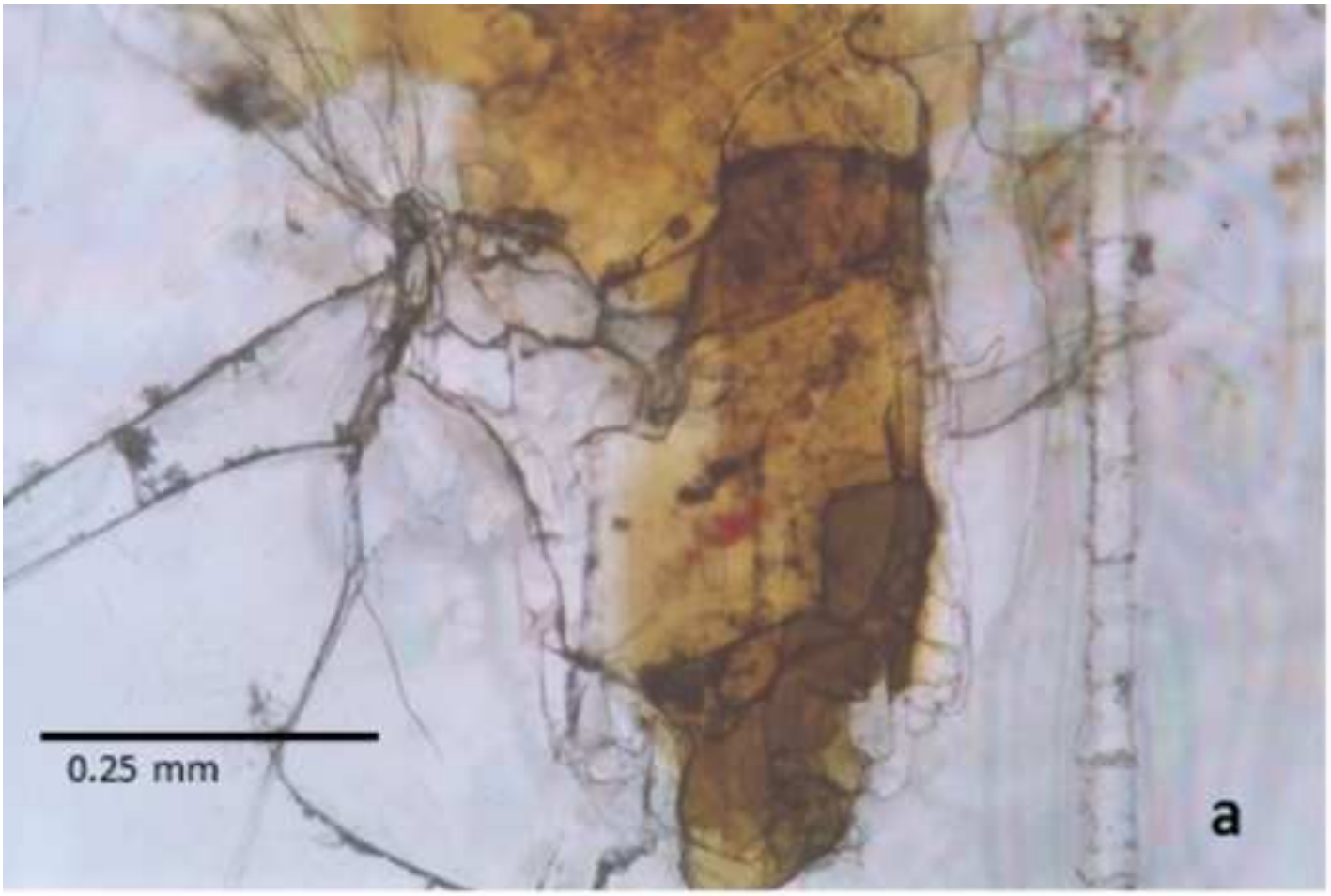

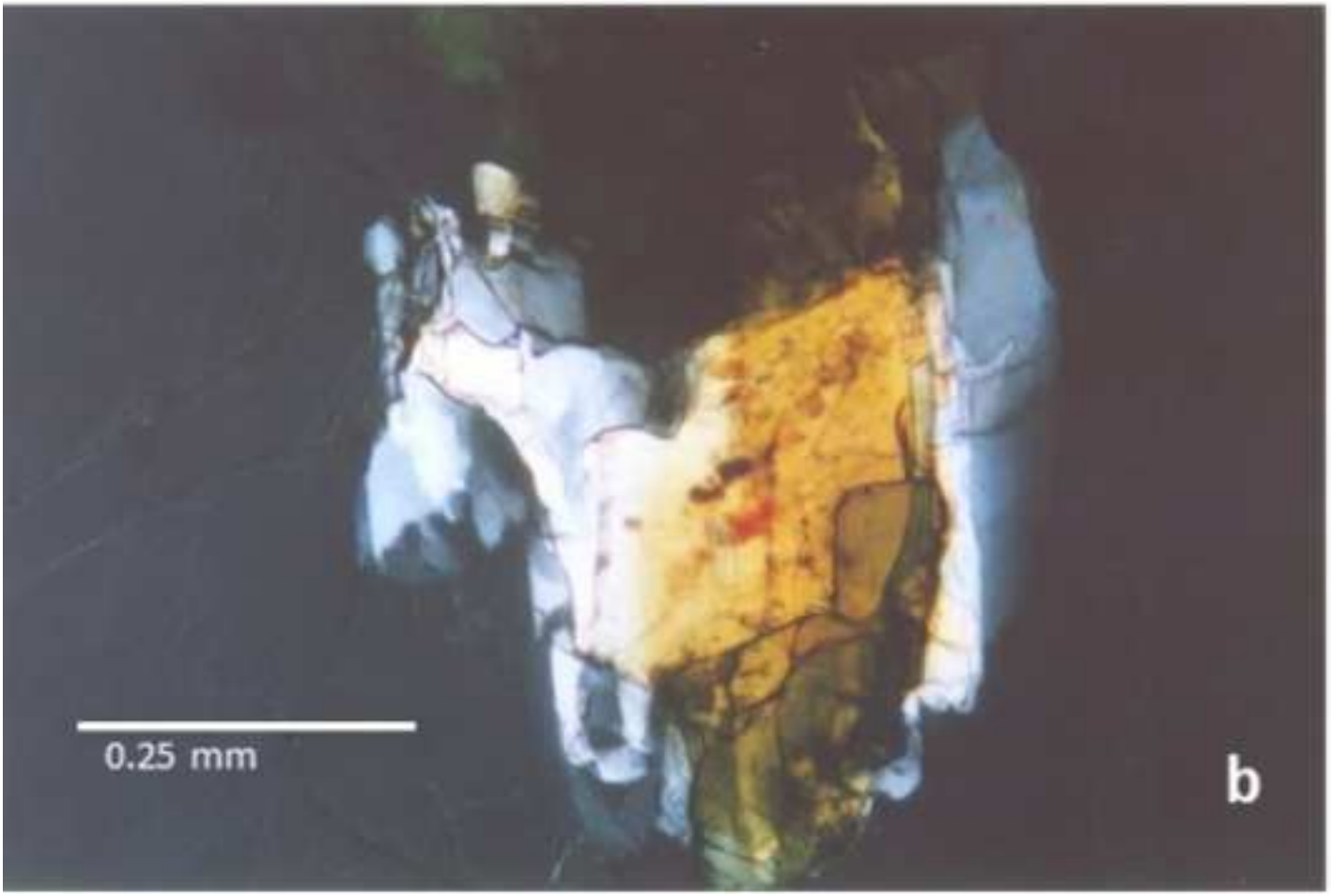

Figure 4

Click here to download high resolution image

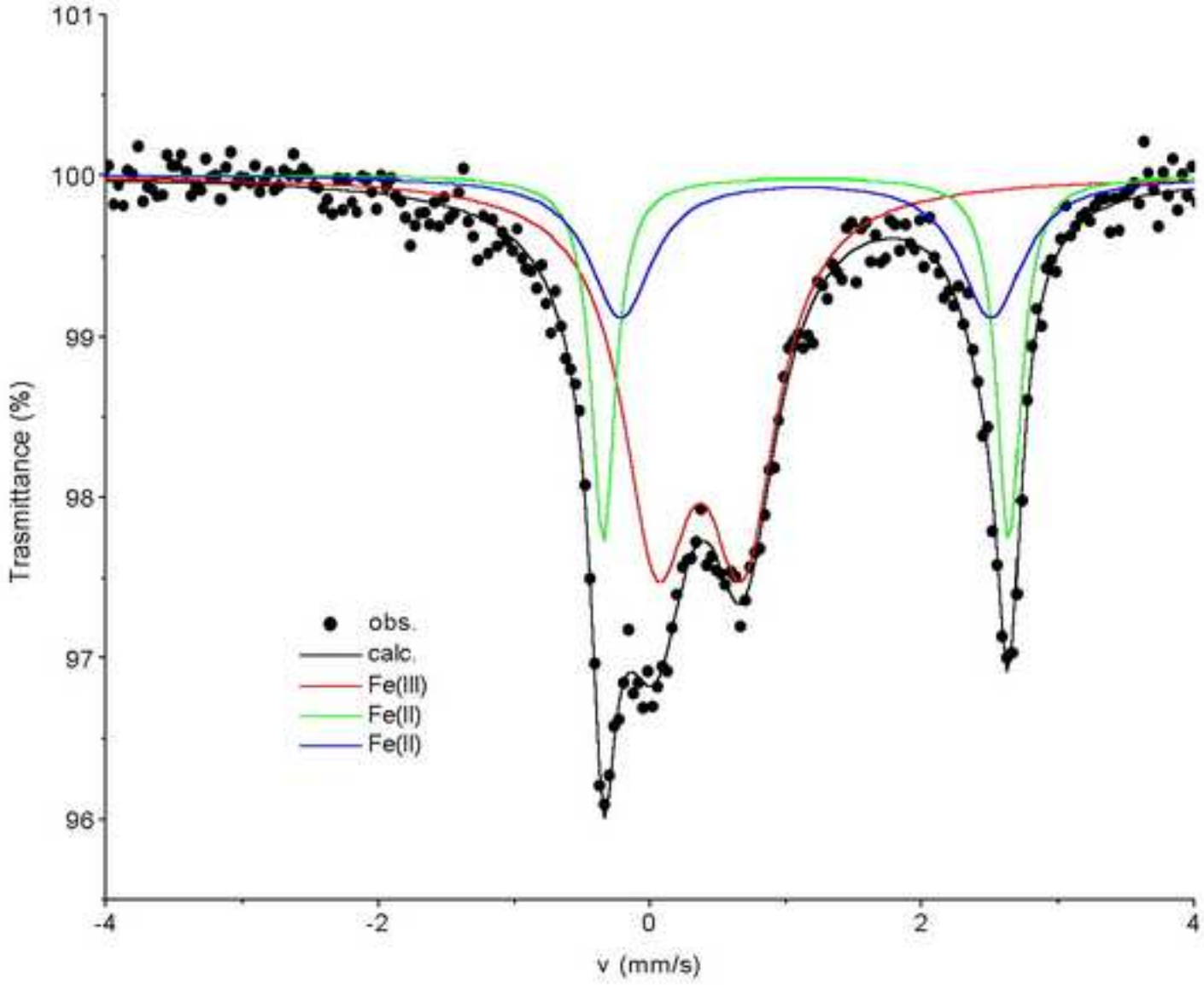

Figure 5

Click here to download high resolution image

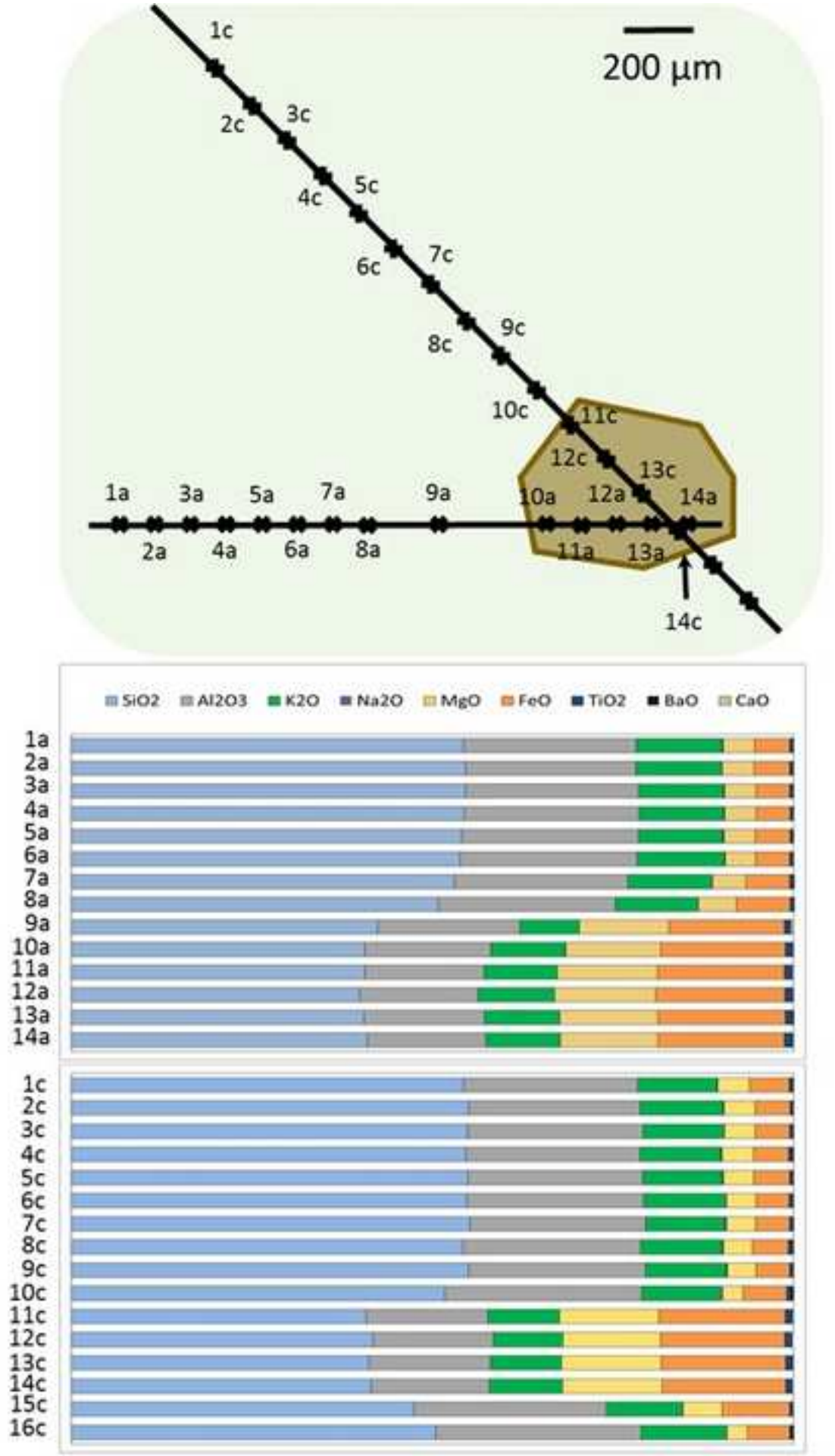

Figure 6

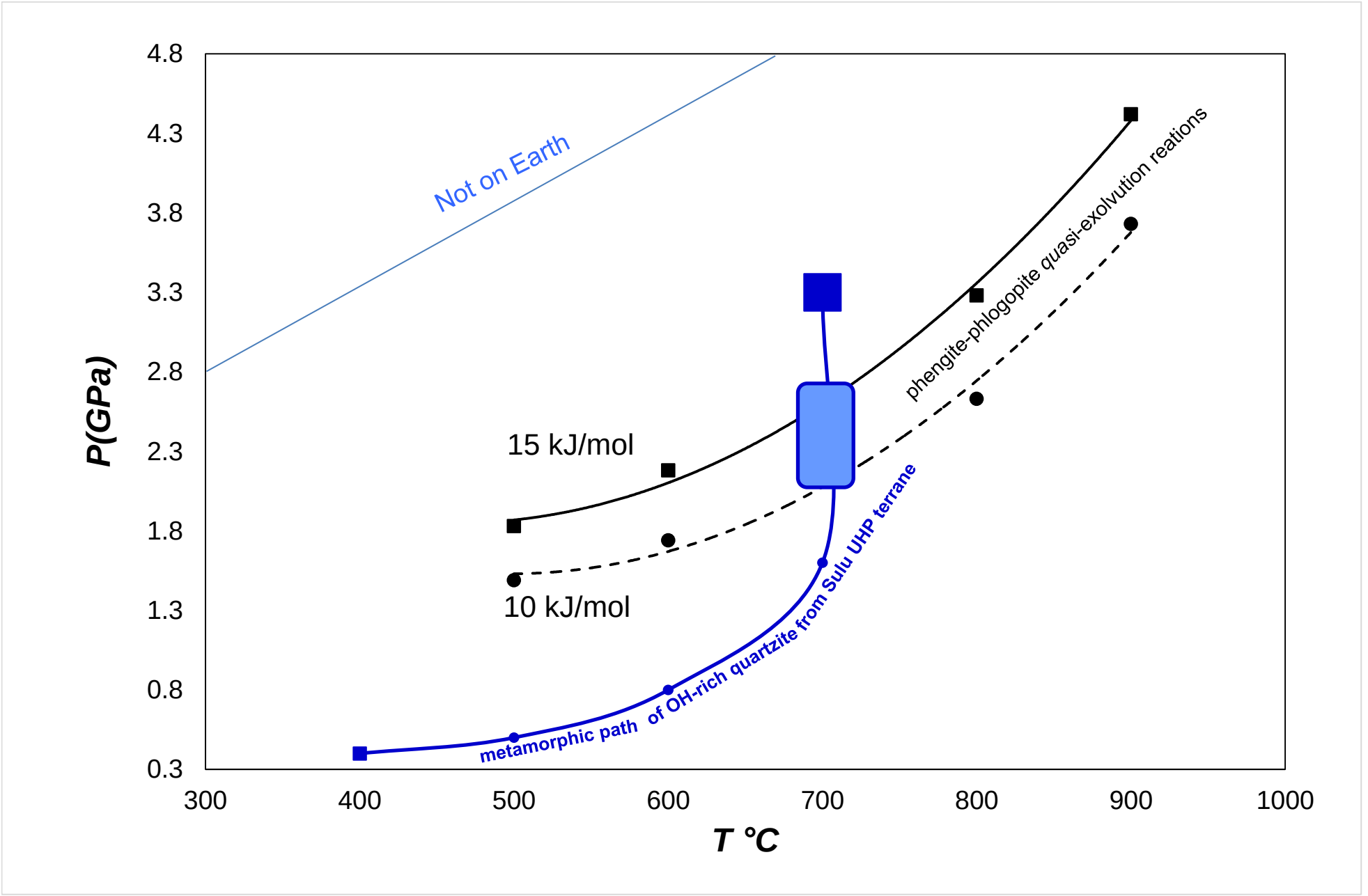
4.8
4.3
3.8
3.3
2.8
2.3
1.8
1.3
0.8
0.3
P(GPa)
300
400
500
600
700
800
900
1000
T °C
Not on Earth
15 kJ/mol
10 kJ/mol
phengite-phlogopite quasi-exolvution reations
metamorphic path of OH-rich quartzite from Sulu UHP terrane

Table 1
Click here to download Table: Table_1.docx

Table 1. Major element analyses (% by weight) of Phe-3T and *quasi*-exsolved Phl-phases determined by EMP

Sample	Phe-3T		phl-3T		phl-1M	
No. of crystals	4		5		9	
No. of analyses	24		15		9	
SiO_2	50.76	(49.00-51.69)	39.35	(38.27-40.50)	37.80	(37.07-38.75)
Al_2O_3	23.44	(21.73-25.04)	15.00	(14.88-15.93)	14.87	(13.98-15.75)
K_2O	10.83	(9.90-11.31)	7.96	(7.69-8.35)	8.76	(8.06-9.98)
Na_2O	0.04	(0.01-0.08)	0.04	(0.00-0.07)	0.03	(0.00-0.08)
CaO	0.00	(0.00-0.00)	0.00	(0.00-0.00)	0.16	(0.10-0.24)
BaO	0.25	(0.16-0.35)	0.03	(0.00-0.16)	0.00	(0.00-0.00)
MgO	4.02	(3.73-4.40)	13.10	(12.70-13.36)	12.58	(12.32-12.81)
FeO	1.92	(1.75-2.21)	14.22	(13.26-14.91)	16.40	(16.03-16.76)
Fe_2O_3	2.53	(2.30-2.94)	-	-	-	-
TiO_2	0.48	(0.42-0.55)	1.10	(0.67-1.29)	0.99	(0.90-1.04)
MnO	0.00	(0.00-0.00)	0.05	(0.00-0.11)	0.07	(0.00-0.13)
F^-	0.00	(0.00-0.00)	0.92	(0.00-1.82)	0.00	(0.00-0.00)
Cl^-	0.00	(0.00-0.00)	0.02	(0.00-0.05)	0.00	(0.00-0.00)
Total	94.27	(90.40-96.78)	92.03	(90.22-93.71)	91.73	(90.73-93.29)
a.p.f.u.						
Si^{4+}	3.46	(3.42-3.55)	2.97	(2.96-3.17)	2.88	(2.84-3.02)
Al^{3+}	1.89	(1.78-1.98)	1.33	(1.31-1.48)	1.33	(1.28-1.44)
K^+	0.94	(0.88-0.99)	0.77	(0.76-0.83)	0.85	(0.80-0.98)
Na^+	0.01	(0.00-0.01)	0.01	(0.00-0.01)	0.00	(0.00-0.01)
Ca^{2+}	0.00	(0.00-0.00)	0.00	(0.00-0.00)	0.01	(0.01-0.02)
Ba^{2+}	0.01	(0.00-0.01)	0.00	(0.00-0.00)	0.00	(0.00-0.00)
Mg^{2+}	0.41	(0.38-0.45)	1.47	(1.43-1.59)	1.43	(1.39-1.49)
Fe^{2+}	0.11	(0.10-0.17)	0.39	(0.36-0.43)	0.45	(0.42-0.48)
Fe^{3+}	0.13	(0.12-0.19)	0.46	(0.41-0.50)	0.53	(0.49-0.56)
Ti^{4+}	0.02	(002-0.03)	0.06	(0.04-0.07)	0.06	(0.05-0.06)
Mn^{2+}	0.00	(0.00-0.00)	0.00	(0.00-0.02)	0.00	(0.00-0.01)
F^-	0.00	(0.00-0.00)	0.22	(0.00-0.47)	0.00	(0.00-0.00)
Cl^-	0.00	(0.00-0.00)	0.00	(0.00-0.01)	0.00	(0.00-0.00)
Σcat	6.98	(6.95-7.02)	7.46	(7.40-7.99)	7.56	(7.51-7.86)
Σcat^{VI}	2.02	(1.99-2.05)	2.69	(2.55-2.98)	2.69	(2.60-2.92)

The a.p.f.u. have been calculated on the basis of 22 negative charges. Fe^{2+} and Fe^{3+} are determined using Mössbauer spectroscopy results (see supplementary materials Table S2)
Maximum and minimum observed values as in brackets; the bottom lines: the sum of total cations (Σcat) and of octahedral cations (Σcat^{VI}).

Table 2
Click here to download Table: Table _2.docx

Table 2: Major element compositions (wt%) of phases and bulk rock used in mass balance calculations.

	Phe-3T	*Phl-3T*	*Phl-1M*	*Qtz	*K-Feld	ASV
SiO_2	54.13	43.35	41.27	100	63.78	76.30
TiO_2	0.51	1.21	1.08		0.00	0.19
Al_2O_3	25.00	16.53	16.24		20.46	13.31
FeO	4.48	15.67	17.91		0.24	2.58
MgO	4.29	14.43	13.74		0.00	1.06
CaO	0.00	0.00	0.17		0.51	0.99
Na_2O	0.04	0.04	0.03		1.53	0.99
K_2O	11.55	8.77	9.56		13.47	4.57

* = quartz (Qtz) and K-feldspar (K-feld) compositions are from metamorphic veins of Sulu -UHP terrains (Wang et al., 2014; Frezzotti et al., 2007)
AVS: bulk rock averaged compositions of Sulu metamorphic veins (Wang et al., 2014; Frezzotti et al 2007)

Supplementary : S1
Single crystal X-ray diffraction data collection and refinement conditions.

	Phe-3T	*phl-3T*	*phl-1M*
a (Å)	5.2248(6)	5.3166(5)	5.3195(13)
b (Å)	-	-	9.2117(12)
c (Å)	29.737(5)	30.21(2)	10.210(3)
β (°)	-	-	100.04(2)
V (Å^3)	703.1(3)	739.00(12)	492.7(2)
Space Group	*P3$_1$12*	*P3$_1$12*	*C2/m*
Z	3	3	2
Radiation	Mo*K*α	Mo*K*α	Mo*K*α
Monochromator	graphite	graphite	graphite
2θ-range (°)	70.00	64.32	70.02
Independ. Refl.	2088	1281	966
$\|F_o\| > 4\sigma(\|F_o\|)$	1828	753	750
Goodness of fit	1.172	2.633	1.066
R $[\|F_o\| > 4\sigma(\|F_o\|)]$	3.50	8.50	4.78
R (all data)	4.34	12.00	8.73
Refined parameters	97	33	57

Table S2.
Mössbauer spectrum refinement results for the sample *Phe-3T*. From left to right: label of the doublet (with reference to Fig.5); chemical shift, δ; quadrupole splitting, ΔE_Q; linewidth, Γ; area proportions of each doublet; attribution to Fe^{2+} and Fe^{3+} corresponding number of atom in a formula unit; * marks the not-refined value.

Doublet	δ *(mm/s)*	ΔE_Q *(mm/s)*	Γ *(mm/s)*	*A (%)*	χ^2	*Attribution*	*a.p.f.u.*
A	0.37±0.01	0.63±0.01	0.60±0.02	57±1	1.00	Fe(III) ott.	0.13
B	1.15±0.01	2.98±0.01	0.21±0.02	21±1		Fe(II) ott.	0.05
C	1.15*	2.73±0.08	0.56±0.07	22±1		Fe(II) ott.	0.06

Table S3 Refined number of electrons (e^-), atom positions (xyz) and isotropic equivalent displacement factors (U_{eq}). *Phe-3T*, first line; *Phl-3T*, second line; *Phl-1M*, third line; esd's values between brackets.

Atom	***e*⁻**	***x***	***y***	***z***	**Ueq**
I	19.2(1)	0.1278(1)	0.2556(2)	0.16667	0.0268(2)
	16.9(2)	0.108(1)	0.217(3)	0.16667	0.0267(9)
	17.85(18)	0.00000	0.50000	0.00000	0.0394(5)
M1	0.3(1)	0.11(3)	0.55(1)	0.00000	-
	-	0.146(2)	0.573(1)	0.00000	0.0100(4)
	14.17(14)	0.00000	0.00000	0.50000	0.0095(3)
M2	14.3(2)	0.7976(2)	0.8988(1)	0.00000	0.0099(3)
	-	0.805(2)	0.9024(9)	0.00000	0.0100(4)
	14.18(12)	0.00000	0.3338(1)	0.50000	0.0090(2)
M3	14.7(2)	0.4550(2)	0.2275(1)	0.00000	0.0104(3)
	-	0.473(3)	0.237(1)	0.00000	0.0100(4)
	-	-	-	-	-
T1	-	0.7863(1)	0.5811(1)	0.09034(2)	0.0099(2)
		0.789(3)	0.559(3)	0.0900(6)	0.0053(4)
		0.0759(2)	0.16716(8)	0.22616(9)	0.0158(2)
T2	-	0.4680(1)	0.9215(1)	0.09037(2)	0.0098(2)
		0.457(2)	0.905(2)	0.0924(4)	0.0053(4)
		-	-	-	-
O1	-	0.6543(5)	0.7773(5)	0.11294(6)	0.0160(3)
		0.648(7)	0.755(6)	0.1103(9)	0.0038(6)
		0.0158(7)	0.00000	0.1705(4)	0.0264(7)
O2	-	0.1272(5)	0.7168(5)	0.10722(6)	0.0172(3)
		0.118(7)	0.690(6)	0.1103(9)	0.0038(6)
		0.3261(5)	0.2297(3)	0.1684(3)	0.0254(5)
O3	-	0.6004(5)	0.2506(6)	0.11251(6)	0.0169(3)
		0.571(7)	0.232(8)	0.109(1)	0.0038(6)
		0.1314(5)	0.1687(2)	0.3912(3)	0.0175(4)
O4	-	0.7513(5)	0.5671(5)	0.03590(6)	0.0138(3)
		0.760(4)	0.559(4)	0.038(1)	0.0038(6)
		0.1286(7)	0.50000	0.3989(4)	0.0200(6)
O5	-	0.5024(5)	0.9406(4)	0.03603(6)	0.0145(3)
		0.521(8)	0.954(9)	0.035(1)	0.0038(6)
		-	-	-	-
O6	-	0.1249(6)	0.1908(5)	0.03492(6)	0.0189(5)
		0.150(4)	0.230(4)	0.036(6)	0.0038(6)
		-	-	-	-
H (*Phe-3T*)	-	0.11(2)	0.32(2)	0.039(3)	0.021(9)

Table S4. Cation-oxygen bond lengths in *Phe-3T*, *Phl-3T* and *Phl-1M*. Estimated standard deviations in parentheses.

	Phe-3T	*Phl-3T*		*Phl-1M*
T1-O1 Å	1.638(2)	1.673(10)	T1-O1 Å	1.6536(12)
T1-O2 Å	1.631(2)	1.638(9)	T1-O2 Å	1.651(2)
T1-O3 Å	1.636(2)	1.649(11)	T1-O2 Å	1.6558(19)
T1-O4 Å	1.619(2)	1.564(11)	T1-O3 Å	1.649(2)
<T1-O> Å	1.631(1)	1.631(10)	<T1-O> Å	1.652(1)
T2-O1 Å	1.616(2)	1.668(10)	-	-
T2-O2 Å	1.638(2)	1.669(9)	-	-
T2-O3 Å	1.631(2)	1.618(4)	-	-
T2-O5 Å	1.638(2)	1.760(20)	-	-
<T2-O> Å	1.631(1)	1.679(10)	-	-
M1-O4 Å (x2)	2.18(7)	2.326(11)	M1-O3 Å (x2)	2.0998(18)
M1-O5 Å (x2)	2.29(7)	2.273(18)	M1-O3 Å (x2)	2.0998(18)
M1-OH Å (x2)	2.202(3)	2.136(15)	M1-OH Å (x2)	2.064(3)
<M1-O> Å	2.22(2)	2.245(10)	<M1-O> Å	2.088(1)
M2-O4 Å (x2)	1.943(2)	2.000(13)	M2-O3 Å (x2)	2.075(2)
M2-O5 Å (x2)	1.951(2)	1.95(3)	M2-O3 Å (x2)	2.078(2)
M2-OH Å (x2)	1.981(2)	2.022(12)	M2-OH Å (x2)	2.030(2)
<M2-O> Å	1.958(1)	1.991(8)	<M2-O> Å	2.061(1)
M3-O4 Å (x2)	1.956(2)	2.077(10)	-	-
M3-O5 Å (x2)	1.966(2)	1.98(3)	-	-
M3-OH Å (x2)	1.994(2)	2.100(9)	-	-
<M3-O> Å	1.972(1)	2.052(8)	-	-
I-O1 Å (x2)	2.980(2)	2.987(6)	I-O1 Å (x2)	2.982(3)
I-O2 Å (x2)	3.016(2)	3.018(9)	I-O2 Å (x2)	2.974(2)
I-O3 Å (x2)	2.981(2)	2.965(14)	I-O2 Å (x2)	2.974(2)
$<I-O>_{in}$ Å	2.992(1)	2.990(4)	$<I-O>_{in}$ Å	2.977(1)
I-O1 Å (x2)	3.143(2)	3.332(6)	I-O1 Å (x2)	3.351(3)
I-O2 Å (x2)	3.279(2)	3.297(7)	I-O2 Å (x2)	3.335(2)
I-O3 Å (x2)	3.156(2)	3.366(14)	I-O2 Å (x2)	3.335(2)
$<I-O>_{out}$ Å	3.193(1)	3.332(4)	$<I-O>_{out}$ Å	3.340(1)
$<I-O>_{tot}$ Å	3.093(1)	3.161(4)	$<I-O>_{tot}$ Å	3.159(1)
$\Delta(I-O)_{in-out}$ Å	0.200(1)	0.342(1)	$\Delta(I-O)_{in-out}$ Å	0.364(1)

Table S5. Sheet thickness and principal distortion parameters in *Phe-3T*, *Phl-3T* and *Phl-1M* . Symbols: Thick: thickness; τ: tetrahedral elongation; α: ditrigonal rotation; Δz: tetrahedral tilting; Δ_{TM}: misfit between T and M sheets; Ψ: octahedral flattening; BLD: bond length distortion; TAV: tetrahedral angle variance; ELD: edge length distortion; J: counter rotation.

	Phe-3T	phl-3T	phl-1M
Thick (T) (Å)	2.241(2)	2.216(8)	2.261(3)
Thick (M) (Å)	2.131(2)	2.212(8)	2.161(3)
Thick (I) (Å)	3.305(2)	3.410(8)	3.453(3)
α (°)	4.48	7.52	8.00
Δz Å	0.15	0.01	0.01
Δ_{TM} Å	0.75	0.71	0.45
τ (T1) (°)	112.12	111.38	110.3
τ (T2) (°)	112.16	109.15	-
BLD% (T1)	0.35	2.05	0.14
BLD% (T2)	0.46	2.42	-
TAV (T1)	9.96	22.84	0.87
TAV (T2)	10.16	37.47	-
ELD% (T1)	1.44	1.80	0.62
ELD% (T2)	1.39	2.93	-
Ψ (M1) (°)	61.38	60.47	58.83
Ψ (M2) (°)	57.04	56.24	58.38
Ψ (M3) (°)	57.31	57.39	-
BLD (M1)(%)	1.98	3.22	0.76
BLD (M2) (%)	0.77	1.36	1.00
BLD (M3) (%)	0.76	2.35	-
BLD (I) (%)	3.23	5.41	2.31
J (M1) (°)	0.53	2.28	0.00
J (M2) (°)	12.19	11.83	0.88
J (M3) (°)	12.70	9.55	-
ELD% (M1)	14.79	6.70	5.31
ELD% (M2)	3.44	4.59	4.53
ELD% (M3)	6.48	5.77	-